# Recent advances in benchtop NMR and its applications

Thomas Castaing-Cordier, Dylan Bouillaud, Jonathan Farjon, Patrick Giraudeau

# Recent advances in benchtop NMR and its applications

Thomas Castaing-Cordier[a], Dylan Bouillaud[a], Jonathan Farjon[a] and Patrick Giraudeau[a,*]

[a]Université de Nantes, CNRS, CEISAM UMR 6230, F-44000 Nantes, France

*Corresponding author: Patrick.giraudeau@univ-nantes.fr

**Abstract:**

Benchtop NMR spectroscopy has known a major growth over the last decade, thanks to the design of permanent, compact magnets in the 1-2 T range, that provide remarkable performance in terms of resolution and sensitivity. Although resulting spectra are more limited than their high-field counterparts, the achievable structural and quantitative information can be maximized by a clever use of pulse sequences –in particular those involving gradient pulses– and by advanced data processing algorithms. In this chapter, we describe the main characteristics of benchtop NMR spectroscopy in 2020, both in terms of hardware and typical performance. We highlight the most recent methodological improvements in the field, in terms of pulse sequences, hyperpolarization and data processing, which have significantly improved the resolution and sensitivity of benchtop NMR spectrometers. Finally, we discuss major applications of benchtop NMR spectroscopy, for reaction and process monitoring, but also for quality control and profiling. The number of papers in this field in the last few years undoubtedly highlights the major role that benchtop NMR has to play for applications in areas such as food and pharmaceutical industry, flow chemistry, and profiling of complex samples.

**Keywords:** NMR spectroscopy, Liquid-state, Benchtop, Compact, Medium-field, Reaction monitoring, Quality control, Profiling

# 1. Introduction

Liquid-state NMR spectroscopy is a general analytical tool that provides powerful information on molecular structure and dynamics, as well as accurate quantitative data on concentration or purity, even in complex mixtures. It has found applications in many fields of science, including chemistry, structural biology, food and plant sciences, pharmaceuticals or forensics. NMR spectroscopy most often relies on high-field superconducting magnets that provide $^{1}H$ resonance frequencies up to 1.2 GHz in 2020 [1], while 300 to 600 MHz spectrometers are now routinely used in many research laboratories and industries. The technological race towards very high $B_0$ fields is easily explained by the properties of NMR spectroscopy, whose sensitivity grows with $B_0^{3/2}$ while its resolution scales linearly with the magnetic field. Increasing $B_0$ obviously provides an efficient way to study increasingly challenging systems, from complex biomolecular systems to biofluids or tissues.

Such performance, however, comes with significant drawbacks mainly stemming from the superconducting nature of high-field NMR magnets, that require bulky and expensive equipment – from a few hundred thousand euros for 400 MHz spectrometers to several millions euros for very high field magnets. Moreover, the need to regularly fill high-field magnets with cryogenic fluids ($N_2$ and He) and the regular hardware maintenance of probes and electronics make their use even more costly. Finally, highly specialized staff are most often associated with the operation of such equipment. All these reasons explain why NMR spectroscopy, in spite of its high potential, is not much visible in our daily life, contrary to alternative analytical methods such as mass spectrometry, near InfraRed (IR) or Raman spectroscopies which have made their way towards hospitals, food industries, and even airports or crime scenes [2–4]. It should be noted, however, that NMR has somehow reached such a level of accessibility through relaxometry equipments which have been used for a long time as portable devices in food or oil industry, for instance [5–7]. But until the 2010s, the accessibility NMR spectroscopy remained limited to research laboratories or relatively big industries.

About a decade ago, the situation started to change with the development of the first benchtop NMR spectrometers [8]. Blümich and co-workers designed the first models, based on a fist-sized Halbach magnet that made the equipment compact enough to be placed under a fume hood, in a teaching lab, or in an industrial setting, while providing a sufficient homogeneity to yield NMR spectra with decent quality. Since then, several companies have been developing such portable NMR spectrometers, and hundreds of them have already been installed in places that were not necessarily accustomed to high-field NMR.

The main characteristics of benchtop NMR spectrometers will be described later in this chapter. However, all of them share common features: a magnetic field between 1 and 2.3 T, a compact electronic system that often fits within the same container as the magnet, the ability to detect most common nuclei (in particular $^{1}H$ and $^{13}C$) with an excellent stability and an impressive linewidth (<0.5 Hz) [9]. Figure 1 shows the most recent commercial instruments from the four manufacturers that sell benchtop NMR equipment in 2020. Although they have a different degree of compactness, all models can fit on a chemist's bench. Benchtop NMR spectrometers are found under different names in the literature, such as "Compact NMR", "Medium-field NMR" or "Low-field NMR". Since the terminology "medium-field" or "low-field" is somewhat arbitrary depending on the reference magnetic field, we will prefer the term "Benchtop NMR" in this chapter.

Benchtop NMR spectroscopy has not been developed to replace high-field NMR, but rather to make NMR accessible in situations where it would be highly needed but which are barely compatible with high field equipments. These include the online monitoring of chemical reactions [10] or biological processes [11], quality control in food or pharmaceutical industry [12,13], but also bringing NMR to teaching labs [14]. Such a broad diversity of applications poses a number of challenges. First –as described later in this chapter– the resolution and sensitivity are much lower than those of high-field spectrometers. Second, targeted samples are often complex mixtures including a great diversity of compounds – in terms of molecular structure and concentration – in non-deuterated solvents. These

limitations have motivated numerous methodological developments – on both signal acquisition and processing sides – to make the most out of benchtop NMR spectrometers. Figure 1 highlights the main areas of methodological developments (hardware, pulse sequences, hyperpolarization and processing) as well as the major application areas.

This chapter first describes the hardware characteristics of benchtop spectrometers, and the typical analytical performance that results from such compact equipment. Then, the recent developments which have helped magnifying the potential of benchtop spectrometers are described in terms of pulse sequences, hyperpolarization and signal processing. Finally, we describe the main application of benchtop NMR spectroscopy: reaction and process monitoring, quality control and profiling. These application encompass diverse fields of science, from industrial chemistry to metabolomics, including food science or forensics.

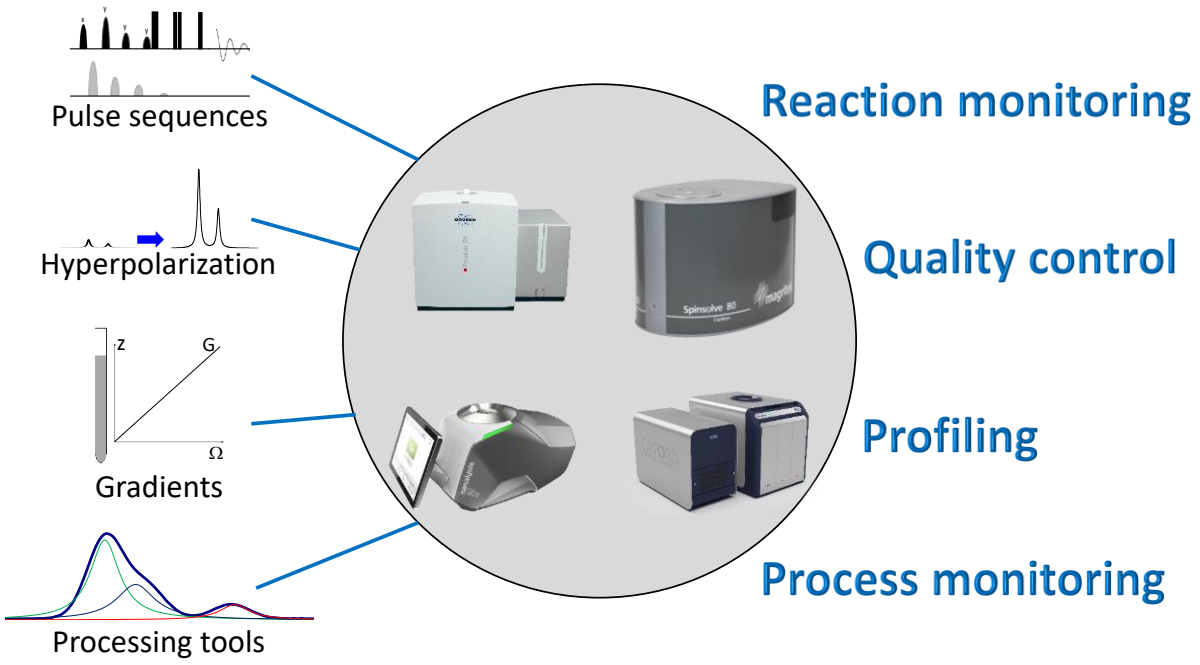


Figure 1. Popular benchtop spectrometers from the four manufacturers that make such equipment available in 2020. The most active areas of methodological development which have been boosting the performance of such equipment are mentioned, as well as the major application areas. Photographs of spectrometers were kindly provided by Bruker Biospin, Magritek, Nanalysis and Oxford Instruments.

# 2. Hardware considerations

## 2.1. Magnets for benchtop spectrometers

Benchtop spectroscopy is a recent technology which has been commercially available for around 10 years [15–19]. Benchtop spectrometers are based on permanent magnetic materials (*e.g.* NdFeB or SmCo [20]), contrary to high-field superconducting magnets that can deliver considerable static magnetic fields (from 5 to 28 T), albeit at the cost of complex equipment (cooling envelops, frequency generators, amplifiers, …) resulting in massive devices. The design and arrangement of permanent magnets have been carefully developed and optimized to ensure magnet field specifications that allow recording NMR spectra with sufficient quality, particularly in terms of magnetic field homogeneity. One can cite the Halbach magnet [21] (Figure 2): a cylindrical array of permanent magnets allowing a homogeneous static magnetic field inside the cylinder. Coupled to an efficient shimming procedure [22], these permanent magnets have become suitable for NMR spectroscopy.

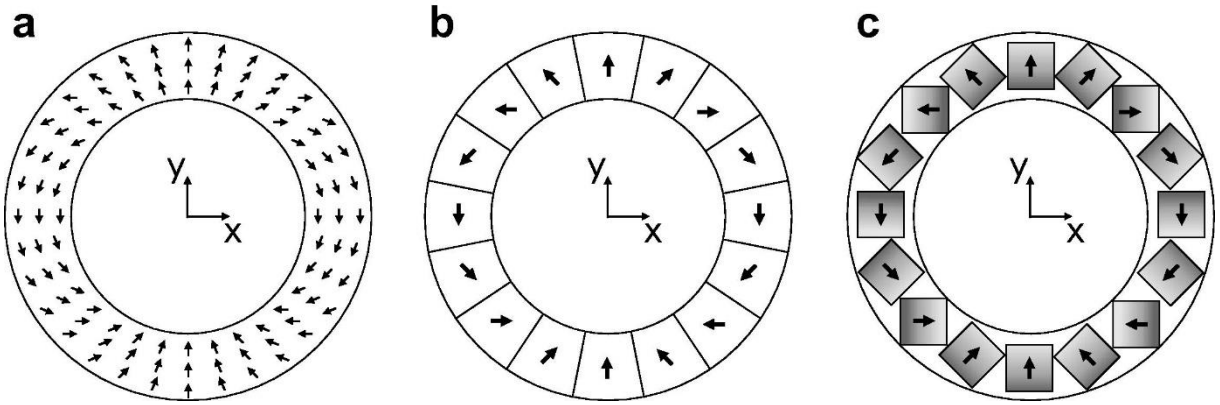


Figure 2. Principle of Halbach magnet design: a cylindrical array of permanent magnets providing a permanent magnetic field along the y direction inside the ring. (a) theoretical Halbach magnet with a continuous evolution of polarization direction along the ring. (b) a possible array of 16 permanent magnets, nevertheless different magnets must be made with different direction. (c) a relevant array of 16 identical permanent magnets. The arrows indicate the polarization direction of each permanent magnet. The x and y axes of the Cartesian coordinate system are centered with the magnet where y points along the direction of the magnetic field. The z axis (not shown) points out of the page. Reproduced with permission from [22].

The main specification of benchtop spectrometers is the strength of the delivered magnetic field, which is often a major sale argument. Magnetic field strength impacts both sensitivity and resolution, as described in the previous section. This results in a race between manufacturers to deliver the highest

magnetic field. In the early 2010s, the first benchtop spectrometers delivered a magnetic field of typically 1 T (corresponding to a $^{1}H$ resonance of 43 MHz). Nowadays, the performance has been more than doubled since the most powerful commercially available benchtop spectrometer delivers a magnetic field of 2.3 T (100 MHz).

The main physical limit in such increase is magnetic field homogeneity. The target Full Width at Half Maximum (FWHM) for high-resolution NMR peaks is below 1 Hz. This involves that magnetic field inhomogeneities must not exceed 1 Hz. For a 1 T spectrometer, this corresponds to a relative homogeneity of $2.10^{-8}$ [23], which is highly demanding. Such performance can be reached through a careful magnet design [22–24] and with a shimming strategy [25]. Commercial benchtop spectrometer achieve a typical FWHM between 0.2 and 1 Hz depending on the device. Such performance is of particular importance at medium magnetic field since it reduces overlap between peaks and provides better peak SNR.

Another crucial specification is the stability over the time of the magnetic field. Benchtop spectrometers, as their high-field counterpart, rely on a field-frequency lock system in order to correct the drift of the magnetic field. Most benchtop spectrometers include an external lock system which makes it possible to analyze samples in non-deuterated compounds. In addition, permanent magnets are very sensitive to temperature variations, hence the latter must be controlled as precisely as possible to avoid large magnetic field variations. To control the magnet temperature, benchtop spectrometers contain regulation systems which also help regulating the sample temperature to a certain extent. Most benchtop spectrometers are designed to work at room temperature but some devices can be heated until 60°C [18,19].

In addition to temperature regulation, a shimming procedure is essential to further correct the magnetic field inhomogeneity. The shims stability over time has been rarely discussed in the literature but is crucial for long acquisition or long monitoring applications. To date, commercial benchtop spectrometers do not include a procedure to automatically adjust the shims in the course of time.

Finally, additional constraints arise from the need to be able to move benchtop spectrometers easily and to set them up in demanding environments (fume hood, chemistry lab or industry), and sometimes in a flow setting (see section 7). Hence, compactness and weight are important requirements. Commercial devices weigh between 20 and 80 kg, making the apparatus more or less convenient to be moved. And compactness is also a major challenge posed to benchtop manufacturers.

### 2.2. Probes and accessories

Benchtop spectrometers can detect various nuclei, depending on the NMR probes included in the hardware configuration. Contrary to high-field NMR spectrometers, users cannot change the probe configuration on a routine basis, due to the compactness of the equipment. As for high-field NMR, $^{1}$H is the most widely detected nuclei, due to both its sensitivity and its occurrence in small organic molecules. However, the detection of $^{1}$H at medium-field suffers from ubiquitous peak overlap and second order coupling effects. $^{19}$F is also a popular nuclei for benchtop NMR, since it is almost as sensitive as $^{1}$H while peaks are spread over a very large frequency range. Moreover, $^{1}$H and $^{19}$F show very close resonance frequencies at medium-field, which makes it possible to detect both nuclei with the same coil without resorting to an additional probe [18]. Reaction monitoring applications on fluorinated compounds have been largely reported with benchtop NMR [26,27]. Depending on the hardware, a second probe can detect a supplementary nucleus such as $^{13}$C or $^{31}$P [28–30]. In addition, the first benchtop spectrometers with a broadband probe have been recently made available, offering an additional flexibility on the observed nucleus and broadening the scope of applications, particularly in organic chemistry [19]. Yet, the detection of additional nuclei mainly remains limited by their receptivity (which takes into account the gyromagnetic ratio and the abundance of the isotope), especially at medium-field. For example $^{13}$C, although a very interesting nuclei for organic molecules, can only be detected in highly concentrated samples at medium-field.

Current benchtop NMR devices are dedicated to liquid-state samples, and to date, no benchtop spectrometer for solid-state NMR detection –for instance with an option of magic-angle spinning– has

been reported. However, Bernard and Michaelis reported $^{207}$Pb spectra of lead salts in a powder form placed inside a benchtop spectrometer, and compared the results to those obtained with a high-field spectrometer [31]. The corresponding spectra (Figure 3) show that chemical shift anisotropy can be detected on a benchtop spectrometer, although the experiment duration –4 days at 1.4 T– makes the application quite impractical. With current hardware, perspectives of benchtop solid-state NMR spectroscopy remain limited to most sensitive nuclei in high concentrations, and the detection of less favorable nuclei such as quadrupolar or low-abundant nuclei remains a long-term perspective. Still, the implementation of magic angle spinning solutions in benchtop hardware could act as a real game changer for solid and semi-solid samples.

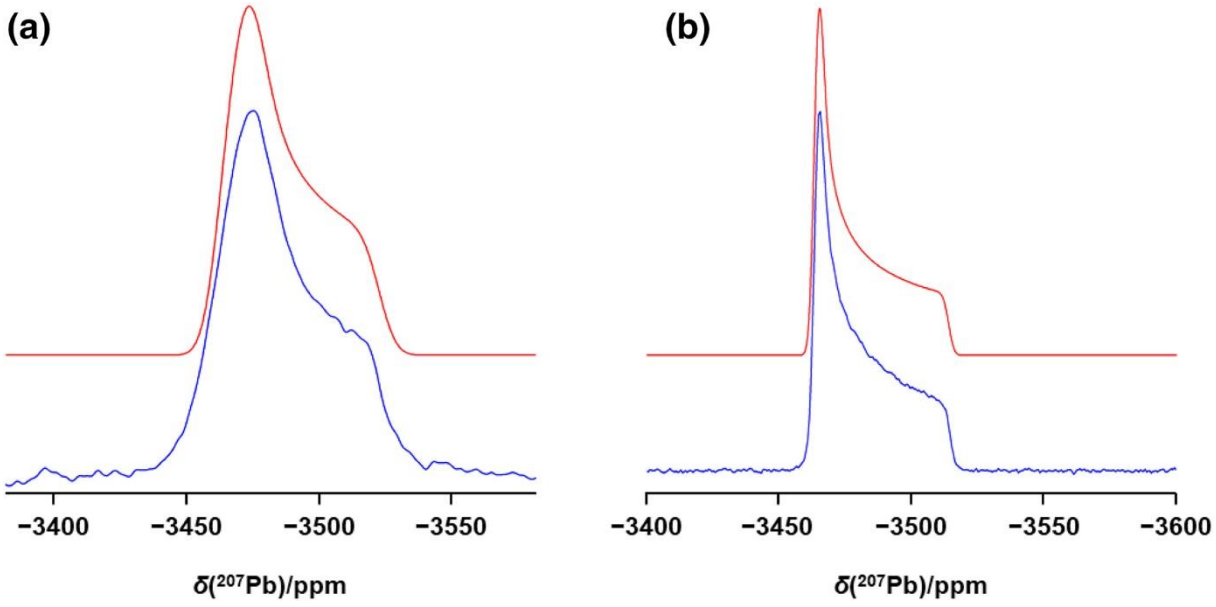


Figure 3. Simulated (upper red trace) and experimental (lower blue trace) $^{207}$Pb nuclear magnetic resonance (NMR) spectra of a nonspinning sample of $PbCl_2$, acquired at 1.4 T (a) and 11.75 T (b) at 305 K. Reproduced with permission from [26].

Back to liquid-state NMR spectroscopy, the addition of a gradient coil in commercial hardware has recently increased the potential of benchtop NMR spectroscopy. Gradient coils are ubiquitous in high-field liquid-state NMR probes, since magnetic field gradients are key ingredients for most high-field NMR pulse sequences, either for coherence-selection purposes, or to implement diffusion-encoded or spatially-encoded experiments. The implementation of gradient coils on benchtop spectrometers enabled researchers to implement pulse sequences including gradient pulses, such as solvent

suppression blocks [32], pure shift [33], ultrafast 2D [34] or diffusion-encoded [35] pulse sequences. These pulse sequences – which can help circumventing some of the drawbacks of benchtop NMR – are further described in Section 4.

Finally, the routine use of benchtop NMR spectrometers, in particular by non-specialists, is limited by the possibility to analyze large series of samples in full automation. To address this challenge, manufacturers have recently developed automated sample changers akin to those used at high-field [15,16]

All benchtop NMR are a compact combination of the hardware elements mentioned above (magnet, shim coils, temperature regulator, transmitter/receiver coil(s), amplifiers, gradients…). Available specifications and accessories are dependent of the brand and the model. The choice between commercially options depends on the targeted application and a comparison between existing commercial models has been recently reviewed by Beek *et al.* [36]. Still, the state-of-the art is rapidly evolving and hardware innovations are regularly released by the manufacturers, who have made tremendous hardware improvements in the last ten years. Further developments are expected in the coming years, therefore a regular literature review would be necessary to remain updated about hardware developments.

# 3. Performance and limitations

### 3.1. Historical perspective

The performance of current benchtop NMR spectrometers is not very different from the results that could be achieved in the early days of NMR – in the 1960s – with the first routine NMR spectrometers. Indeed at that time, common NMR spectrometers did not exceed 100 MHz. Figure 4 shows a 1D $^{1}$H spectrum dating from 1969 on a morpholin derivative [37], highlighting the limited resolution and sensitivity at this field. Peak assignment and structure elucidation were not as easy as they are now

with high-field spectrometers. While the spectral quality of current benchtop NMR spectrometers has been significantly improved compared to these initial spectra, intrinsic limitations remain. Issues of resolution and sensitivity are still present. However, the electronics has been greatly improved since 1960, the shims and electronics are more efficient (Section 2). The 1960 spectrometers were much more bulky whereas benchtop NMR takes very little space since it can be directly installed on a bench. Figure 5 shows a 1D $^{1}$H spectrum of ibuprofen at 312 mM obtained at 60 MHz on a benchtop spectrometer, highlighting the improved spectral quality compared to initial benchtop spectrometers.

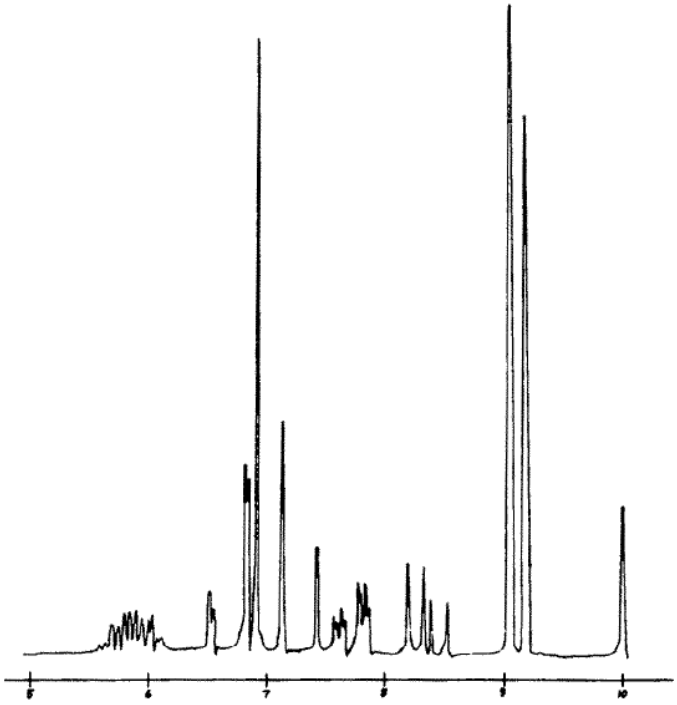

Figure 4. The 1D $^{1}$H spectrum of N-benzyl 6-methyl morpholin-2-one (III, R = benzyl). Reproduced with permission from ref [37].

### 3.2. Spectroscopic features

To illustrate the typical spectral quality that can be obtained with modern benchtop NMR spectrometers, a comparison was performed between a typical middle-range high-field NMR spectrometer (400 MHz spectrometer) and a 60 MHz benchtop spectrometer. The corresponding $^{1}$H spectra, for a concentrated ibuprofen sample, are shown in Figure 5.

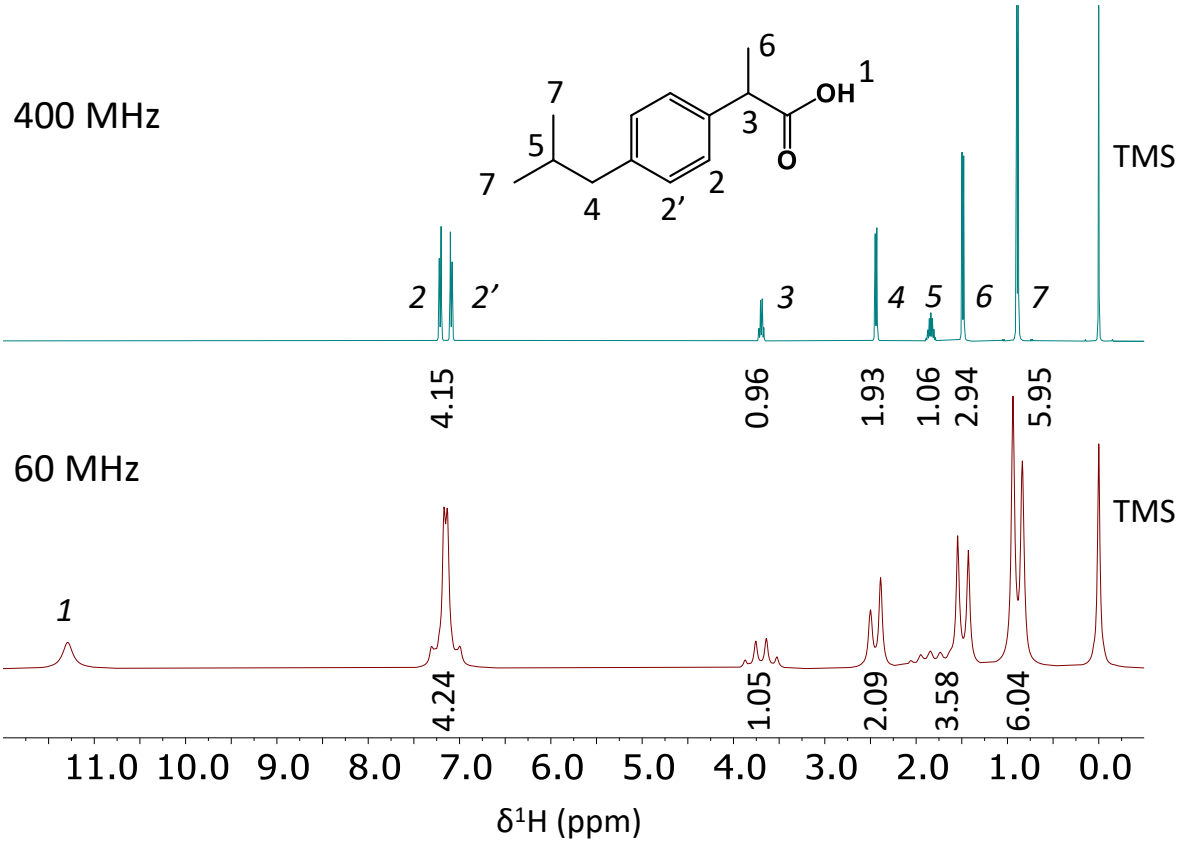


Figure 5. Spectrum of a 312 mM ibuprofen in $CDCl_3$ at high-field (400 MHz) and on a benchtop spectrometer (60 MHz). Peak integration after phasing and baseline correction are indicated under the peaks. Peak numbering is indicated in italics. The two spectra are obtained with the same conditions: 8 scans, a repetition time (TR) of 30 s and an acquisition time of 1.6 s.

Since the resolution scales linearly with $B_0$ in theory, the 400 MHz spectrum is expected to be 12 times more resolved than at 60 MHz. However, in practice, the ratio is more in favor of benchtop NMR for two reasons. First, benchtop spectrometers can reach a better $B_0$ homogeneity than their high-field counterparts, with a FWMH lower than 1.2 Hz at 60 MHz and 3 Hz at 400 MHz on a $D_2O/H_2O$ reference tube. This can be attributed to a different shim coil design, as well as the effect of radiation damping at high field, in the case of concentrated samples. Still, the separation of peaks is much less favorable at medium field, due to the limited spectral range in Hz. This leads to major peak overlap that can be detrimental to the identification and quantification of peaks. In terms of sensitivity, the theoretical ratio of sensitivity between two devices could in principle be calculated by the ratio of the $B_0^{3/2}$. In the example of Figure 5, a 400 MHz spectrum should be in theory 17 times more sensitive than a 60 MHz recorded in identical conditions. SNR evaluation of Figure 5 data provides a factor of 16, close to this

theoretical value. Finally, the comparison of 400 MHz and 60 MHz spectra highlights the ubiquitous second order coupling effects (or strong coupling) at medium field. Strong couplings appear when $\Delta\delta^{1}H$ are smaller or equal to $J_{HH}$, therefore they are much more observed at medium magnetic field.

### 3.3. Quantitative performance

To illustrate the ability of benchtop spectrometers to provide reliable quantitative data, a relative integration was carried out by fixing the total integration at 17 $^{1}H$. It was possible to integrate signals 2 to 7 of the ibuprofen molecule, however signals 5 and 6 were highly overlapped. More generally, peak tails were more or less overlapped due to the limited spectral range, making the integration quite difficult. This resulted in an average difference of 17% between integrals obtained at 400 and 60 MHz. This illustrates that benchtop NMR can provide fairly accurate relative integration except when signals are overlapped. This drawback could be circumvented by the use of spectral deconvolution tools [38,39], although this could be less suited to routine analysis by non-experts. Concentration determination by benchtop NMR (qNMR) could also be performed, in principle, following the same rules as at high-field NMR, but its practical use may be limited by peak overlap [40].

Also worth discussing is the performance of benchtop NMR spectrometers in terms of limits of detection (LOD) and quantification (LOQ). The LOD represents a resonance intensity which is 3 times the background noise value, and the LOQ corresponds to a ratio of 10 times this noise level [41]. Both LOD and LOQ are functions of the magnetic field. The detection and quantification limits are directly related to the strength of the magnetic field, but the shape and sharpness of the peaks also greatly affect the quality of the integral measurement. Thus, the higher the resolution of the spectrometer, the lower the LOD and LOQ [42]. A first study was carried out in flux on a 43 MHz spectrometer and showed a LOD close to 3 mM and a LOQ of 10 mM within a single scan [20]. Another work on the analysis of dietary supplements revealed that the observable quantitation limit was of the order of 2.0 mM with an experiment time of 45 min on 60 MHz $^{1}H$ [43]. As a comparison, at high magnetic fields (400 MHz), it is typically possible to detect quantities around 0.005 mM and to quantify around 0.05

mM in 4 minutes [44]. At higher fields, analytes at micromolar concentrations can easily be detected, such as metabolites in biofluids [45]. To summarize, at fields below 100 MHz, the detection and quantification limits are close to mM, whereas for a high magnetic field most commonly encountered (400 MHz) it is possible to detect concentration close to µM and to quantify concentrations of a few dozen of µM.

### 3.4 Structure elucidation capabilities

The emergence of benchtop NMR spectrometers has raised major expectations from the chemistry community in terms of structure elucidation capabilities. Structure elucidation generally relies on a set of multi-dimensional experiments, which are available in routine on commercial spectrometers. For the sake of comparison, we acquired a set of such typical 2D spectra at both high and medium magnetic field (Figure 6): $^{1}$H-$^{1}$H COrrelated SpectroscopY (COSY) (Figure 6.A), $^{1}$H-$^{13}$C Multiplicity Edited (ME) Heteronuclear Single Quantum Coherence (HSQC) (Figure 6.B) and $^{1}$H-$^{13}$C Heteronuclear Multiple Bond Correlation (HMBC) maps (Figure 6.C). Note that similar experiment times were chosen for this comparison, benchtop spectra required more scans (due to the lower sensitivity) and less $t_1$ increments (due to the smaller spectral range) than their conventional counterparts. On the COSY spectrum, most of the important correlations for structural elucidation can be observed, in particular the correlation between the two $CH_3$ and the nearby CH (blue circle in Figure 6.A). However, the 60 MHz map has a lower resolution than the 400MHz. So, it is much more difficult to differentiate the two types of aromatics which are strongly coupled in 1D $^{1}$H. Moreover, the aliphatic zone presents overlapped correlations that would make a structure elucidation task quite difficult.

For $^{1}$H-$^{13}$C HSQC, a multiplicity edition was used to provide information on the degree of protonation of all carbons (Figure 6.B). The 60 MHz map shows all the expected correlations for non-quaternary carbons of the molecule and provides the correct substitution for each of them. However, the aromatic protons are very difficult to discern on the medium field spectrum since they appear at the same $^{1}$H

chemical shift due to strong coupling. Their differentiation is only made using the carbon dimension (red circles in Figure 6.B).

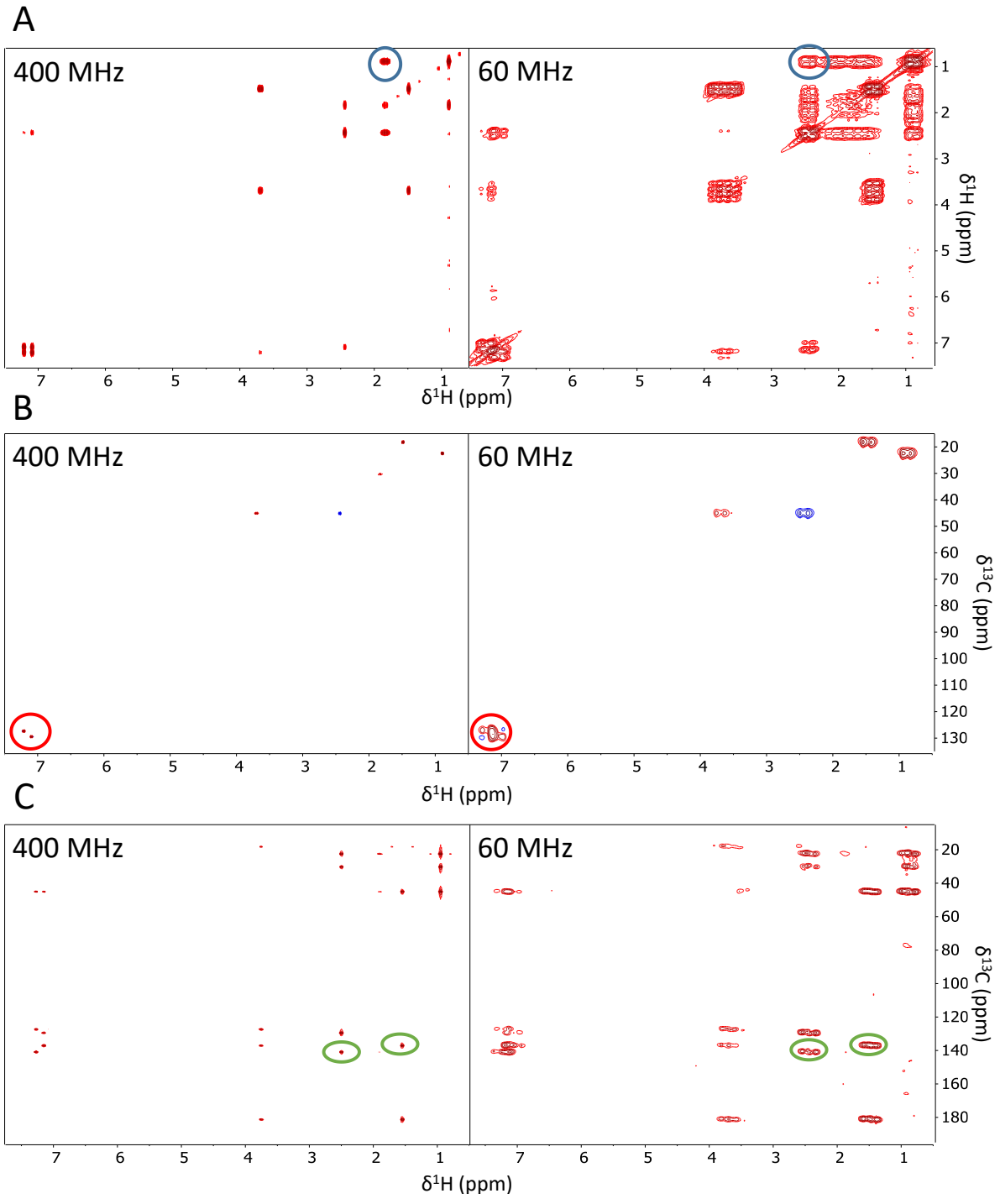


Figure 6. A) $^{1}$H-$^{1}$H COSY B) $^{1}$H-$^{13}$C HSQC C) $^{1}$H-$^{13}$C HMBC obtained on a 400 MHz (left column) and a 60 MHz (right column) spectrometer, for a 312 mM ibuprofen sample in DMSO-$d_6$. 400 MHz acquisitions: $^{1}$H-$^{1}$H COSY obtained with 512 $t_1$ increments, TR = 2 s and 2 scans (34 minutes); $^{1}$H-$^{13}$C HSQC obtained wit 512 $t_1$ increments, TR = 2 s and 2 scans (34 minutes); $^{1}$H-$^{13}$C HMBC obtained wit 512 $t_1$ increments, TR = 2 s and 8 scans (136 minutes). 60 MHz acquisitions: $^{1}$H-$^{1}$H COSY obtained with 512 $t_1$ increments, TR = 2 s and 4 scans (68

minutes); $^{1}H$-$^{13}C$ HSQC with 128 $t_1$ increments, TR = 2 s and 24 scans (102 minutes); $^{1}H$-$^{13}C$ HMBC with 256 $t_1$ increments, TR = 2 s and 24 scans (205 minutes).

Finally, $^{1}H$-$^{13}C$ HMBC is one of the most powerful techniques since it allows to obtain long-distance heteronuclear information on the whole molecular structure (Figure 6.C). Classically, $^{1}H$-$^{13}C$ HMBC is superimposed with $^{1}H$-$^{13}C$ HSQC to obtain the totality of the heteronuclear information of the molecule. The maps recorded with the two fields allow to obtain similar information, indeed most of the correlations are found in the two maps. In particular the correlations circled in green which allows to link the $CH_3$ and the CH with the aromatic ring.

The three pulse sequences described above make it possible to obtain a complete structural elucidation of the molecule regardless of the magnetic field. However, the comparison was carried out on a relatively simple structure and on a concentrated sample. For more complex systems, the use of benchtop NMR will most likely be limited by both resolution and sensitivity issues. Still, as for high-field NMR structure elucidation, other pulse sequences may be used to remove ambiguities such as TOtal Correlated SpectroscopY (TOCSY). TOCSY can be particularly useful at medium field since individual spectra of each spin system can be better discriminated. For example, this pulse sequence has been used for the structural elucidation of strychnine on a benchtop spectrometer [46]. If a problem of 3D structure determination arises, the J-resolved sequence could be used to determine the coupling constants between atoms in the $F_1$ dimension and obtain information on bond angles. Pulse sequences providing information on dipolar couplings such as Rotating frame Overhauser Effect SpectroscopY (ROESY), Nuclear Overhauser Effect SpectroscopY (NOESY) and Heteronuclear NOESY (HOESY) could also be used at medium field to determine the relative configuration of an alkene (Z or E), an asymmetric carbon (R or S) in diastereoisomers but also to get insight into conformational and / or chemical exchanges between atoms. To the best of our knowledge, none of the pulse sequences of this family have been used at medium magnetic field, probably for sensitivity reasons. Figure 7 lists all the pulse sequences that could be used in principle to carry out structural elucidation, bearing in mind that it is often necessary on a benchtop spectrometer to record a larger number of spectra than at

high field, to get rid of ambiguities arising from peak overlaps. Finally, most of the heteronuclear pulse sequences described above are often performed on carbon but it is also possible to apply them to other nuclei. For instance, Gouilleux *et al.* used a $^{1}H$-$^{31}P$ TOCSY to describe a mixture of several phospholipids [28].

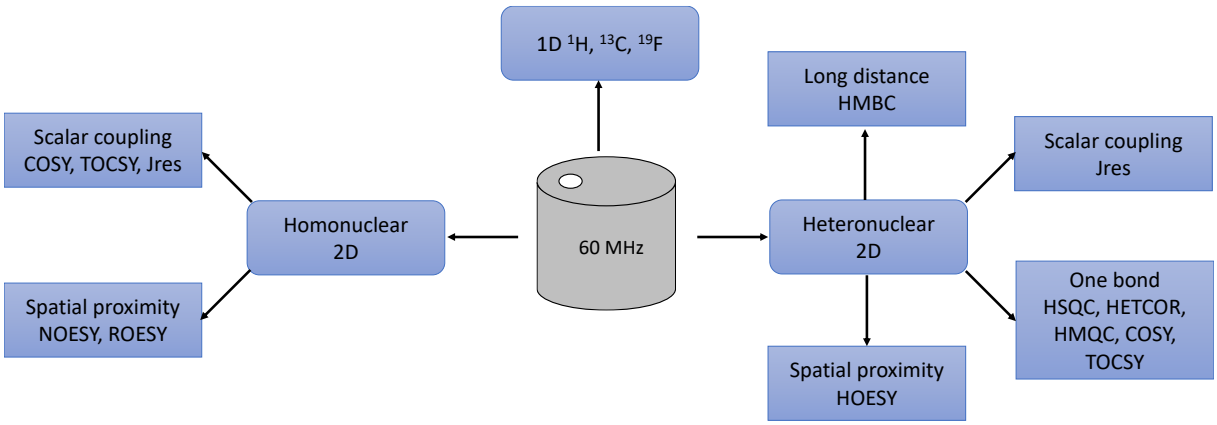


Figure 7. Pulse sequences available for structure elucidation at medium magnetic field.

This performance evaluation reveals a number of limitations that could arise at field strengths under 100 MHz, such as signal overlap leading to difficulties in accurately determining chemical shifts, and of course a lower sensitivity. Therefore, the NMR community has developed various solutions to circumvent these limitations, by using either more advanced pulse sequences (section 4) or signal processing methods (section 5).

## 4. Pulse sequence advances

On compact instruments, the spectral resolution is severely limited by the narrow frequency range that generates ubiquitous peak overlap and strong coupling effects. Pulse sequence developments have been carried out in recent years to better separate overlapping peaks arising from complex mixture components (analytes and/or solvents). Most of these developments rely on the addition of a gradient coil (as mentioned in Section 2) enabling the application of gradient pulses, but also on the pulse sequence programming capabilities offered by manufacturers. This section focuses on such developments, including solvent suppression schemes, diffusion-encoded methods like diffusion-

ordered spectroscopy (DOSY), and spatially-encoded experiments like ultrafast (UF) and pure-shift methods.

### 4.1. Solvent Elimination Schemes

At medium magnetic field, detecting the $^{1}H$ signals of the analytes can be made difficult by strong and numerous peak overlaps with intense solvent signals, particularly when non-deuterated solvents are used. In addition to this overlap issue, the detection of smaller peaks is further hampered by the limited dynamic range of the receiver that is optimized for bigger signals. In the field of chemical synthesis, the use of solvent mixtures worsens this problem. In the case of biological samples, the strong water signal is also a major issue since such an intense signal prevents the detection of close smaller signals and is the main source of baseline perturbation which highly affects the phase of signals belonging to the analyte of interest (Figure 8).

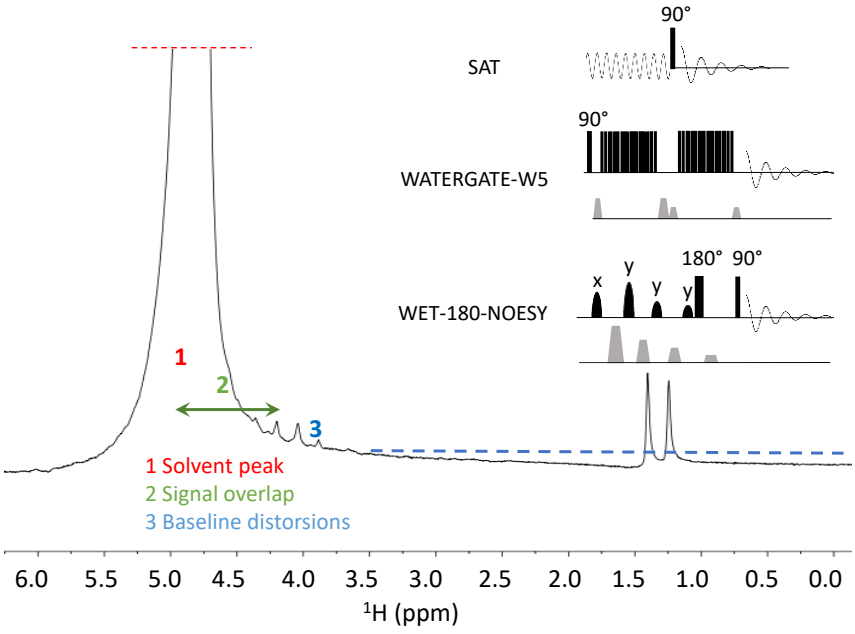


Figure 8. Typical issues arising from strong solvent signals at medium-field (200 mM lactate sample in $H_2O$). 1) The strong solvent peak saturates the dynamic range of the receiver; 2) it overlaps with analyte signals and 3) generates a baseline distortion. Some typical pulse sequences that can be implemented on a benchtop spectrometer to deal with these issues: continuous-wave presaturation (Sat), WET-180-NOESY and WATERGATE-W5.

Various dedicated blocks can be used to suppress the solvent signals. Some of them rely on the saturation of the solvent magnetization before detecting the signal from the analytes. This is the case

of continuous-wave presaturation (Sat) [47] and of the schemes based on the WET pulse sequence [48] such as WET-180-NOESY [49]. Others rely on a selective refocusing of the analytes' magnetization after excitation, such as the WATER suppression by GrAdient Tailored Excitation (WATERGATE)-based pulse sequences [50]. They have already been commonly and intensively utilized at high magnetic fields. The efficiency of these schemes is based on 1) their ability to reduce the intensity of the solvent signal(s), 2) the selectivity of this suppression, i.e., the ability to preserve nearby signals and 3) their quantitative performance, evaluated from the trueness and precision for the peaks of interest.

Reaching good signal suppressions is made difficult by radiation damping effects on big solvent signals [51]. Moreover, the faraway solvent is another obstacle for eliminating unwanted signals [52]. This phenomenon is due to spins located on the edge of the rf coil, which undergo a slightly different $B_0$ field and contribute to enlarge solvent signals. The impact of such effects has been widely described at high magnetic field, but benchtop NMR has its own particularities. On the one hand, even if faraway solvent effects are still present, radiation damping is a less important issue as compared to high-field NMR. On the other hand, the narrow spectral range makes it more difficult to achieve a high selectivity for solvent suppression. Moreover, additional overlap could possibly occur between signals of interest and $^{13}C$ satellites of some organic solvents. Finally, for flow samples, shorter pulse sequences are expected to be less sensitive to flow effects (see section 7).

At high magnetic field, the simplest and easiest method to implement solvent suppression scheme is the well-known continuous wave presaturation [47]. However, under flow conditions, Sat is not the most suitable scheme since not compatible with the long saturation delay occurring in the recycling time. Moreover, such a long time prevents the detection of protons in exchange with the solvent making analysis less informative for water-soluble biological samples. Under such conditions, gradient-based solvent elimination schemes are more interesting, and with the assistance of a gradient coil, most relevant gradient-based pulse methods were implemented on a benchtop spectrometer [32,53].

For small molecules, the performance of different solvent suppression techniques at 43 MHz was assessed by Gouilleux *et al.* [32] under static and flow conditions, in protonated water. Figure 9 shows typical spectra resulting from such evaluation for lactate, which is a challenging case at medium field since the quadruplet corresponding to the methine of lactate is only 30 Hz away from water at 43 MHz. While the Sat scheme is hampered by a lack of selectivity, the WET pulse sequence [48] is more efficient on this criterion, however the baseline is impacted by faraway water. Some variants of the WET pulse sequence are more robust to face faraway water impacts such as WET-CP and WET-180 [52]. These schemes yield to a fully resolved quadruplet of the lactate CH signal. A flat baseline is also visible with NOESY 1D scheme [49]. On the contrary, excitation sculpted schemes such as WATERGATE [50] or excitation-sculpting (ES) [54] are less suitable for small molecules: although the solvent signal is perfectly removed, J-modulation effects appear during the pulse sequence and unfortunately affect the phase and intensity of the signals. Among all explored techniques, the WET-180-NOESY was considered as the most efficient combination for small molecules at medium-field, since it offers a very good quantitative performance, including flow conditions [32].

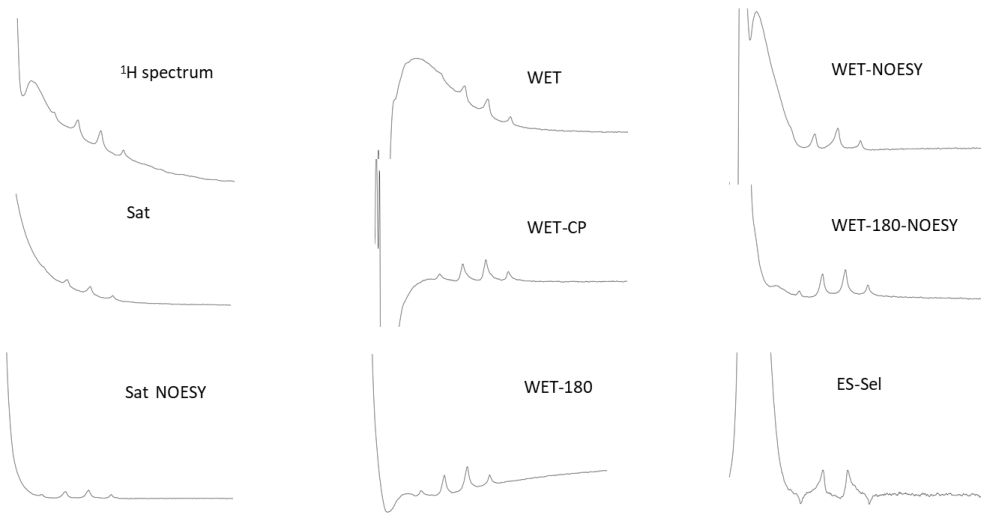


Figure 9. Different schemes performance on a lactate sample in water at 43 MHz. Sat: presaturation; CP: composite pulse; WET: water suppression enhanced by T1 effects; ES: excitation-sculpting; Sel: selective. Reproduced with permission from [32].

In the previously described case, the suppression selectivity was the main problem but sensitivity was not an issue since the lactate was highly concentrated at 0.2 mol.L$^{-1}$. At a lower concentration, pulse

sequences yielding more efficient solvent suppression may be needed even if they are less selective. Bouillaud *et al.* compared the aforementioned solvent suppression methods to probe lipids in aqueous samples, for lipid-concentrated microalgae cells studied under flow conditions [55]. Selectivity was less critical in this case since the target total lipid $CH_2$ peak was 150 Hz away from the water signal, with a low concentration (9 $mg.L^{-1}$). With this kind of sample, WET-180-NOESY was not efficient enough to reduce the water signal –by 37 as compared to $^1H$– for the most sensitive detection of the lipid signal (Figure 10). On the contrary, WATERGATE-5 pulse sequence provided better results allowing a reduction by 27,000 of the $^1H$ water signal. The intrinsic J-modulation effects of this pulse sequence were not a severe obstacle here since the lipidic signal at 1.2 ppm (Figure 10) was relatively broad.

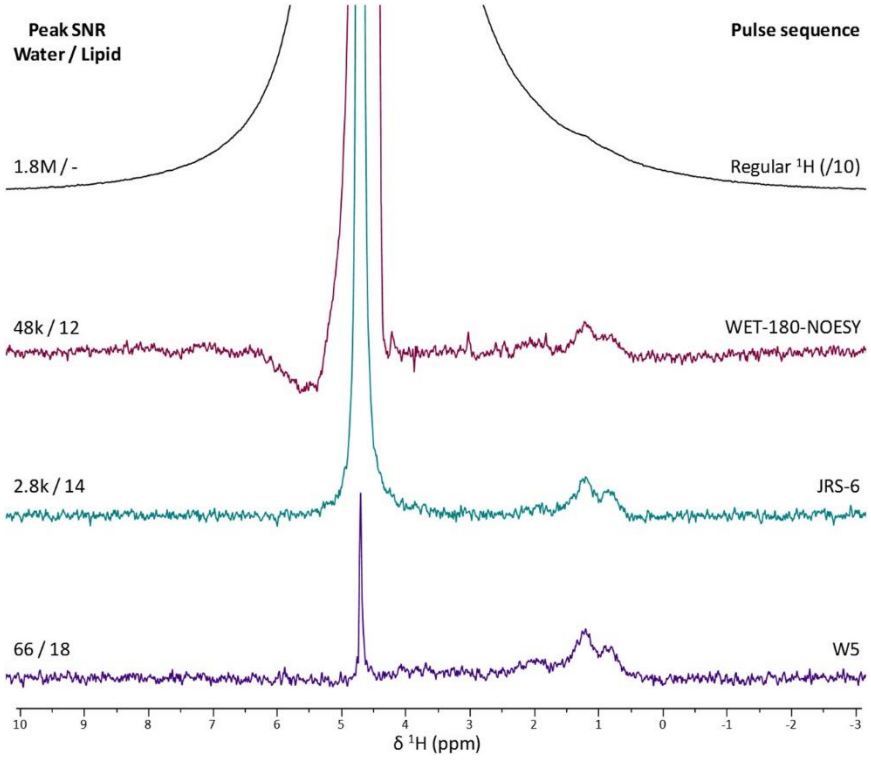


Figure 10. Evaluation of water suppression pulse sequences on a benchtop spectrometer, on non-starved concentrated *Parachlorella kessleri*. From top to bottom: regular $^1H$ spectrum (the water peak is so intense that the spectrum intensity has been divided by 10); the WET-180-NOESY spectrum; the JRS-6 spectrum and the W5 spectrum. A manual baseline correction has been applied for the four spectra. Residual water peaks are visible at 4.7 ppm. The efficiency of the water peak reduction was taken into account as the main criterion for choosing the pulse sequence. Figure reproduced with permissions from [55].

When multiple solvent signals need to be removed, the combination of several solvent suppression techniques may be needed. This can be the case in the field of reaction monitoring, where mixtures of

protonated solvents are often used, leading to numerous intense signals. For instance, Legros *et al.* combined a Sat scheme with a WET-180-NOESY pulse sequence to remove simultaneously two strong solvent signals in a depolluting process monitored on line with benchtop NMR [56]. While a gradient coil appears as an essential ingredient to suppress solvent signals, some benchtop spectrometers may not offer such possibility, and alternative methods can be implemented. In the field of polymeric mixture analysis, a hyphenated method composed on a size exclusion chromatographic device with a medium-field NMR instrument was implemented. To remove the eluting solvent signal, a $T_1$ filter pulse sequence was used with a post processing protocol to reduce signals of eluting solvent by 500 and to enhance the sensitivity for polymeric signal of interest [57,58].

### 4.2. Diffusion-encoded pulse sequences

Diffusion-encoded techniques have become an essential tool for the analysis of complex mixtures, the investigation of dynamic events and determination of the molecular weight [59,60]. The most popular way of plotting such diffusion-encoded data is Diffusion-Ordered Spectroscopy (DOSY). Also known as chromatographic NMR, this tool is well established on high-field NMR instruments, but it is also very promising for benchtop NMR. With the emergence of gradient-equipped benchtop spectrometers, the implementation of diffusion-encoded pulse sequences has become possible.

DOSY techniques rely on a pseudo-2D acquisition mode gathering a series of NMR experiments based on Pulsed Field Gradient Stimulated Echo (PFGSTE) or Pulsed Field Gradient Spin-Echo (PFGSE) recorded with increasing gradient amplitudes. Under a restricted diffusion regime in the absence of convection, the signal amplitude decays as the gradient amplitude increases at a rate described by the Stejskal-Tanner equation [59]:

$$I = I_0 e^{-D(\gamma g \delta)^2 \Delta} \qquad \text{eq. 1}$$

Where *I* is the signal intensity that is attenuated by the application of a gradient, $I_0$ is the signal intensity observed in the absence of gradient, *D* is the translational diffusion coefficient of the considered

compound, $\gamma$ is the gyromagnetic ratio, $\delta$ is the gradient duration, $\Delta$ is the diffusion time and $g$ corresponds to the amplitude of the pulse-field-gradient.

In practice, the DOSY map is obtained by fitting the signal decay to eq. 1. Numerous multivariate models have been developed for such procedure [61]. The resulting lineshape strongly depends on the quality of the fit, and the fitting procedure is made even more critical by peak overlaps in the spectral dimension, which is particularly critical at medium-field.

Nevertheless, promising results were recently obtained in two independent studies (Figure 11). Assemat *et al.* showed that PFGSTE followed by a Longitudinal Eddy current Delay or LED block yielded diffusion-weighted spectra with good line-shape and flat baseline [60]. Carney *et al.* used a variant of PFGSTE called Oneshot45 [62] with additional gradient pulses and a final one 45° pulse to reduce the impact of J-modulation (Figure 11.C). This approach was able to accurately determine the weight of different polymers by correlating diffusion coefficients to hydrodynamic radii [63].

Another main feature of DOSY experiments is the type of gradient ramp through the pseudo 2D acquisition mode. In the case of a mixture of small and big-sized due to slow and faster diffusion, different ramps were considered and a semi-Gaussian ramp was found to lead to the better alignment of signals for a given diffusion coefficient [60].

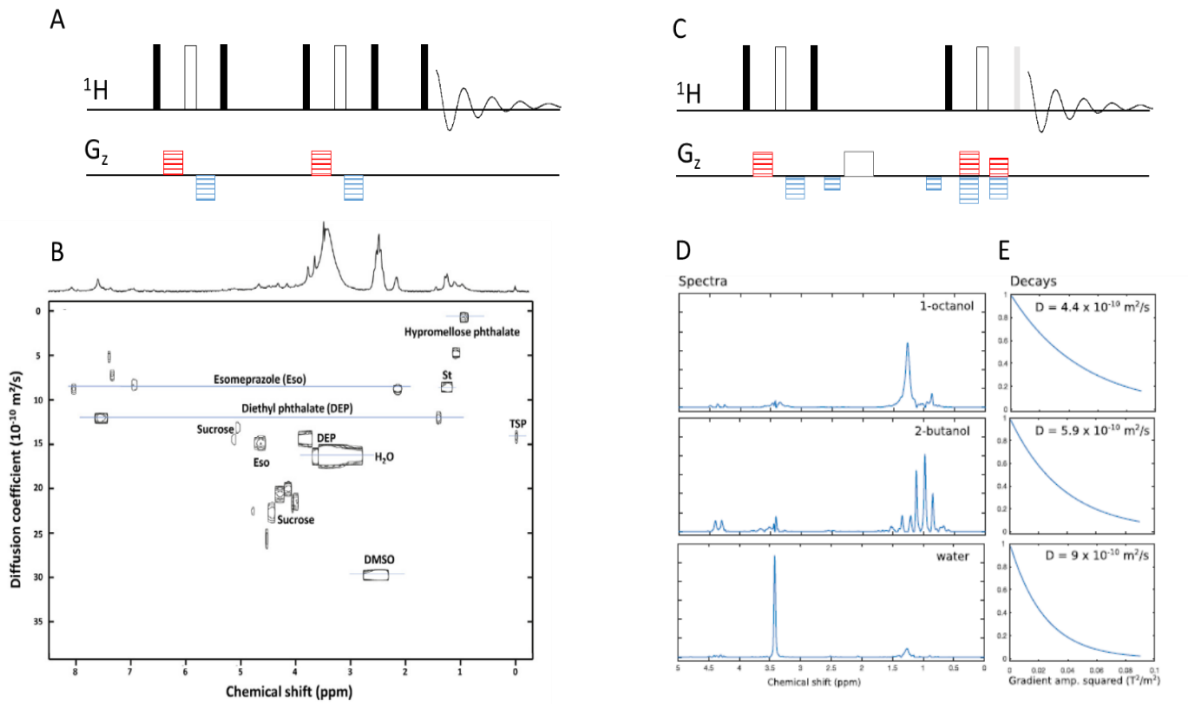


Figure 11. DOSY pulse sequences implemented on a benchtop spectrometers and subsequent results, A) The bipolar pulse pair-stimulated echo-longitudinal eddy current delay scheme or BPPSTE-LED, B) DOSY map obtained with this pulse sequence on a commercial sample of esomeprazole (Ranbaxy) in DMSO-d6 at 43 MHz and processed with a univariate processing whereby lines automatically peak-picked were fitted to a mono-exponential decay. Reproduced with permission from [60] .C) Oneshot45 pulse sequence allowing to record a 2D DOSY with no J-modulation. D) Extracted spectra from the SCORE processing with E) diffusion coefficients for a mixture of 2-butanol, 1-octanol and water; data recorded with pulse sequence C). Reproduced with permission from [64]. Black, white and grey rectangles correspond to 90°, 180° and 45° hard pulses. Red and blue dashed rectangles are positive and negative pulse field gradients respectively.

After data acquisition, diffusion-encoded data can be processed either with univariate or multivariate approaches. Univariate processing consists in fitting eq. 1 by assuming that signals are well-resolved along the horizontal axis, where they correspond to a single diffusion coefficient. On the contrary, multivariate processing does not require any prior hypothesis on peak overlap but requires prior knowledge on the number of molecules in the sample. Assemat *et al.* showed that with limited peak overlap, univariate processing was sufficient to obtain reliable diffusion coefficients as compared to high-field DOSY maps [60] (Figure 11.B). Mc Carney *et al.* proposed to struggle against severely overlapped DOSY spectra with a multivariate processing strategy applied to a mixture of two alcohols whose 1D spectra showed strong peak overlap [64]. Their approach, based on the SCORE algorithm, showed reliable diffusion coefficients with a good differentiation of the components in the mixture, as shown on Figure 11 D & E. Investigating other multivariate techniques such as PARAllel FACtor analysis

(PARAFAC) [61], Maximum Entropy [65], LOcal COvariance order DOSY (LOCODOSY) [66] or Direct Exponential Curve Resolution Algorithm (DECRA) [67] would be interesting to potentially improve the potential of benchtop NMR DOSY.

### 4.3. Spatially-encoded techniques

At high magnetic field, major methodological advances have been made over the last two decades thanks to the development of spatially-encoded techniques that found inspiration in Magnetic Resonance Imaging (MRI). These spatially-encoded methods, mainly developed in high-resolution liquid-state NMR spectroscopy [68] rely on the combination of frequency-selective or frequency-swept pulses combined with pulse field gradients. Thanks to the implementation of a gradient coil and to the pulse programming capability of modern benchtop NMR instruments, spatially-encoded pulse sequences have been successfully implemented on compact spectrometers.

#### 4.3.1. Ultrafast 2D NMR

The primary spatially-encoded scheme which was implemented on a benchtop spectrometer is UF (or single-scan) 2D NMR, introduced in 2002 by Frydman and co-workers in 2002 [69]. The UF pulse sequence has the same structure as conventional multi-dimensional experiments, however the conventional time-incremented period is substituted by a spatial encoding period where a helicoidal magnetization winding is generated by simultaneously applying linearly frequency-swept pulses with gradients (in blue Figure 12.A) [70]. During the acquisition time, this information is decoded with an Echo-Planar Spectroscopic Imaging scheme (EPSI, in pink Figure 12.A). After appropriate data rearrangement and processing, a 2D spectrum is obtained in a single scan. Thanks to its single-scan character, UF 2D NMR was successfully applied to a variety of situations where short acquisition durations where needed, from the real-time monitoring of fast chemical or biochemical reactions, to the detection of 2D spectra of hyperpolarized mixtures [71]. UF suffers from sensitivity limitations mainly associated with large digital filter bandwidth that needs to be applied during acquisition due to the frequency dispersion coming from gradients. In addition, UF NMR requires compromising between

spectral width and resolution, and pulse sequence improvements have been suggested to face these limitations [71]. In addition, multi-scan techniques based on UF 2D NMR have been shown to advantageously replace conventional 2D NMR in high-throughput metabolomics [72].

Ultrafast 2D NMR was the first gradient-based pulse sequence to be implemented on a benchtop spectrometer in 2015 [73]. Clean 2D UF COSY spectra recorded in only 400 ms showed lineshapes close to the simulated spectra. The quality of the spectrum shown in Figure 12.B highlights the suitability of the UF NMR experiments at medium-field, and the performance of the gradient coil and amplifier. While the inherent low sensitivity of the benchtop spectrometer was worsen with the sensitivity losses inherent to UF 2D NMR, reasonable signal averaging made it possible to reach a limit of detection lower than 500 mM in less than 1 minute of experiment (Figure 12.C) [34]. Such UF 2D COSY experiments achieved an excellent repeatability (<3%), paving the way to applications in reaction monitoring and profiling which are described in the next Sections of this chapter.

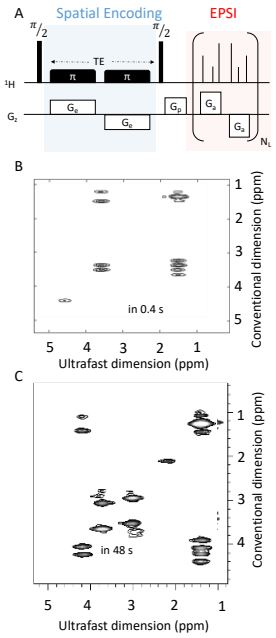


Figure 12. UF 2D COSY pulse sequence A) and corresponding spectrum B) of a sample of ethanol in $D_2O$, recorded in 0.4 s in a single-scan and C) of ethylbromopropionate at 1 mol.L-1 in acetone-$d_6$ in 12 scans, on a 43 MHz benchtop spectrometer. The ”ultrafast” axis refers to the spatially-encoded dimension (without Fourier transformation) whereas the ”conventional” axis represents the direct dimension. TE: duration of spatial encoding; Ge: amplitude of spatial encoding gradients; Gp: amplitude of pre-acquisition gradient; Ga:

amplitude of acquisition gradient; NL: number of loops for the EPSI scheme applied during the signal detection. Figure adapted and reproduced with permission from [34].

#### 4.3.2. Pure-shift NMR

Another promising ensemble of techniques to simplify the analysis of complex mixtures is pure-shift NMR, which improves the spectral resolution of 1D or 2D spectra by removing $^{1}$H-$^{1}$H couplings in the $^{1}$H dimension [74]. The first approach to record pure-shift spectra was based on the projection of J-resolved 2D spectra after a 45° tilt procedure, an approach that was, however, impacted by phase-twisted lineshapes [75]. This method was recently used on a benchtop spectrometer to obtain homodecoupled 2D COSY spectra after processing by Generalized Indirect Covariance (GIC) [76].

More recently, pure-shift NMR enjoyed a revival through the development of spatially-encoded methods that combine selective, band-selective, or frequency swept chirp pulses with gradients so that coupling partners in a spin system are excited in different slices of the sample [74,77]. Such methods are becoming increasingly popular at high-field, but have only been implemented for the first time in 2019 on a benchtop spectrometer. Castaing-Cordier *et al.* showed that a variety of well-known pure-shift methods, such as Zangger-Sterk or Pure-Shift Yielded by Chirp Excitation (PSYCHE) pulse sequence families, could be implemented and provided efficient broadband homonuclear decoupling (Figure 13) [33]. However, pure-shift NMR spectra at 43 MHz suffered from reduced sensitivity as already described at higher fields. In addition, while strong couplings are a limitation of pure-shift NMR at high-field, this becomes much more effective at medium-field, where strong coupling effects are predominant, even for simple spin systems.

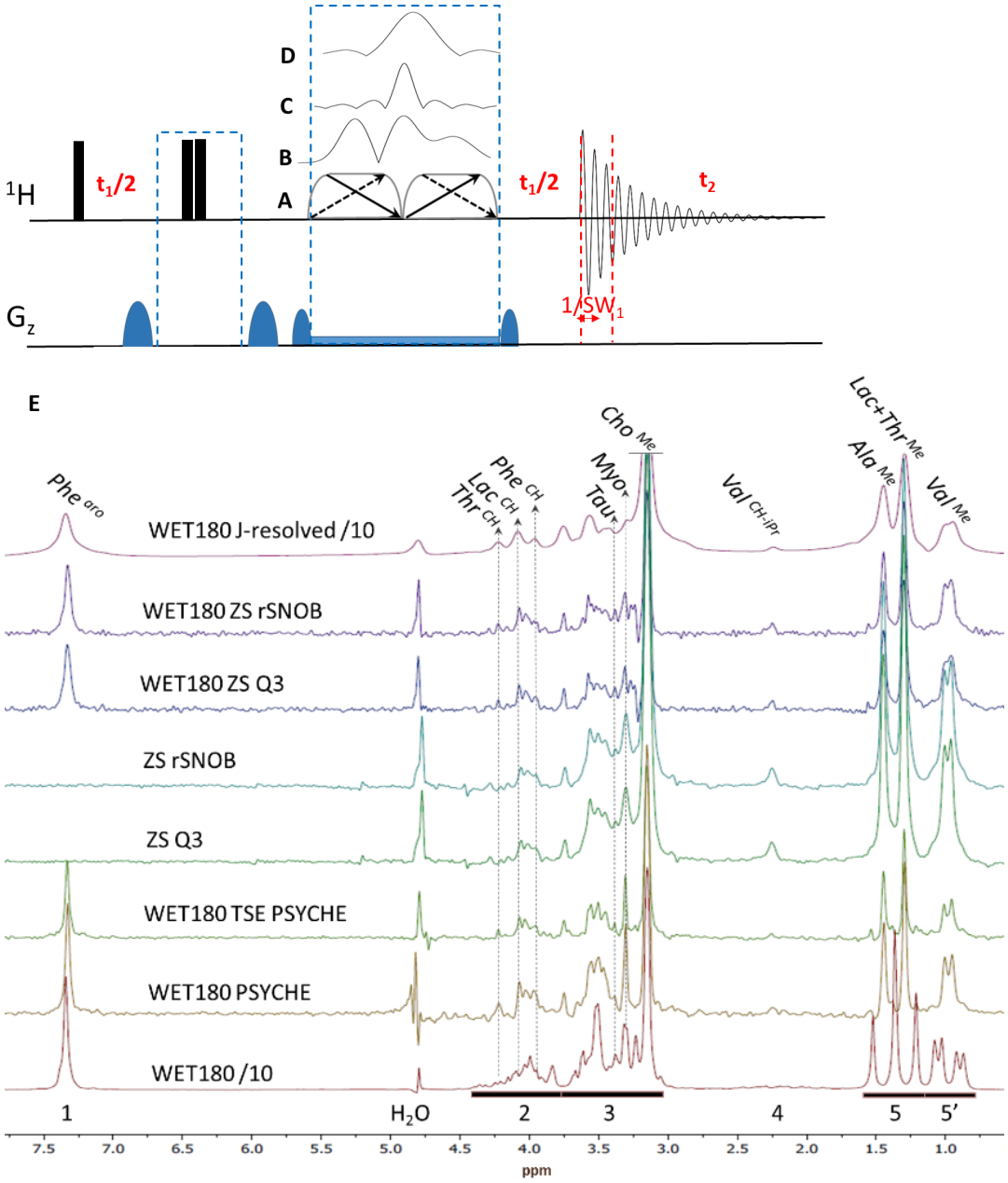


Figure 13. Pulse sequences for pure-shift $^1$H experiments with pseudo-2D acquisition mode. Double spin echo based methods: PSYCHE pulse sequence (A), Zangger-Sterk (ZS) pulse sequences with a Q3 (B) ReBURP (C) and rSNOB (D) 180° refocusing selective pulse. (E) Example of different pure-shift spectrum acquired with A, B, C, D, Triple Spin Echo (TSE) PSYCHE and J-resolved sequences for $J_{HH}$ decoupling as compared to the standard 1D $^1$H spectrum. Spectra were recorded in 28 min on an 8 metabolite mixture: Alanine (Ala), Choline (Cho), Lactate (Lac), Myoinositol (Myo), Phenylalanine (Phe), Taurine (Tau), Threonine (Thr) and Valine (Val) with at least one assigned signal per metabolite on the top. For all techniques, a WET-180 scheme has been used prior to the sequence, except for ZS experiments with a reduced frequency sweep. Figure adapted with permissions from [33].

Overall, PSYCHE provided the most efficient decoupling for $^1$H multiplets, leading to a resolution improvement by a factor 2 to 3 and a slightly better sensitivity than ZS methods. On the contrary, the latter were found more efficient to decouple broad multiplets. The authors also noticed a very good

repeatability for these pulse sequences (<5%) [33]. Applications have not been yet described, but regarding the spectral simplification capabilities of pure-shift NMR, it is envisionable to expect applications for profiling and monitoring similar to those targeted by UF 2D NMR, focusing on highly-concentrated or even hyperpolarized samples. Additional perspectives could also come from 2D pure-shift experiments, whose implementation on a benchtop spectrometer was reported by Blümich and Singh [46]. Since such techniques are based on a natural abundance $^{13}C$ BIlinear Rotation Decoupling (BIRD) filter, they are not hampered by sensitivity losses as compared to the conventional version like other ZS and PSYCHE schemes and have a nice capability to make easier the spectral analysis of complex mixtures.

# 5. Hyperpolarization and benchtop NMR

As described in previous sections, benchtop NMR suffers from a limited sensitivity compared to high-field NMR, which is not the most sensitive analytical method itself. Indeed, NMR spectroscopy has a low sensitivity owing to the poor nuclear spin polarization in a magnetic field at thermal equilibrium. The NMR sensitivity is directly proportional to the Boltzmann polarization. At high-field, such polarization is already very low (*e.g.* $7.6\ 10^{-6}$ for $^{1}H$ at 300 K in a 14.1 T field), but becomes even lower on a benchtop spectrometer (*e.g.* $8.3\ 10^{-7}$ for $^{1}H$ at 300 K in a 1.5 T field). And the situation is of course even worse for nuclei with a lower magnetic ratio such as $^{13}C$. In such context, hyperpolarization methods which have revolutionized high-field NMR and MRI could be equally beneficial to benchtop NMR spectroscopy. Indeed, such approaches can produce nuclear spin polarization far beyond thermal equilibrium, resulting in sensitivity improvements by several orders of magnitude. Most popular methods for applications to chemistry are dynamic nuclear polarization (DNP) [78] and Para-Hydrogen Induced Polarization (PHIP) [79]. In addition to their ability to strongly enhance benchtop NMR signals, there are several reasons why the combination of benchtop NMR with hyperpolarization could be even more promising. First, flow and/or portable hyperpolarization settings are emerging, that could make PHIP or DNP particularly compatible with the transportable character of benchtop NMR. Second,

compact spectrometers can be brought closer to the hyperpolarization source, thus limiting polarization losses between hyperpolarization and NMR detection. Recent proof-of-concepts showing the promising combination of benchtop NMR with hyperpolarization are discussed in this section, as well as the perspectives arising from such combination.

### 5.1. Dynamic Nuclear polarization

DNP was originally proposed by Overhauser in 1953 and its first experimental verification was carried out by Carver and Slichter on metallic lithium. DNP relies on the transfer of polarization from electron spins to nuclear spins thanks to a microwave irradiation of the Electron Paramagnetic Resonance (EPR) transitions. Since the electron spin polarization is much higher than the one of nuclei (it reaches almost unity at low temperatures in a magnetic field of a few T), the DNP phenomenon can boost the sensitivity of NMR detection by several orders of magnitude, both in liquids and solids [80].

For liquid-state NMR spectroscopy, a first approach to DNP consists in performing the polarization transfer directly in the liquid-state [81]. This method, known as Overhauser DNP (O-DNP) provides modest signal enhancements since the electron to nuclei polarization transfer mechanisms are relatively inefficient. Still, this approach could offer a convenient way to improve *in situ* the sensitivity of benchtop NMR detection. Such a perspective was recently explored by Lee *et al.*, who developed a benchtop O-DNP-NMR system based on a permanent magnet of 1.6 T, reporting signal enhancement factors between 7 and 40 for simple molecules such as ethanol or water [82].

However, the most efficient and popular DNP method in liquid-state NMR spectroscopy is dissolution DNP (d-DNP) proposed by Ardenkjaer-Larsen *et al*. in 2003 [83]. It is a two-magnet approach where the sample is first polarized in a glassy state at low temperatures (a few K) upon microwave irradiation in a medium magnetic field (3 to 7 T). Frozen hyperpolarized samples are then rapidly dissolved in a superheated solvent and transferred to an NMR spectrometer where regular liquid-state pulse sequences can be applied. The advantage of this approach is that it provides huge sensitivity enhancements arising not only from the DNP process, but also from the temperature jump between

polarization (at a few K) and detection (at ambient temperature). However, such hyperpolarization rapidly decreases upon $T_1$ relaxation during the transfer step, with typical lifetimes of a few tens of seconds for slow-relaxing nuclei. Moreover, the irreversible character of the dissolution process makes it poorly suited to record multi-scan experiments. Still, the tremendous sensitivity gains offered by this method – up to $10^5$ for slow-relaxing quaternary carbons – have revolutionized entire application fields, in particular pre-clinical or clinical MRI [84]. In liquid-state NMR spectroscopy, d-DNP has opened many new application perspectives in reaction monitoring, metabolomics, or ligand-protein interaction studies [85].

So far, there has been only one study reporting the combination of d-DNP with benchtop NMR. The reason is probably that d-DNP requires heavy and high-cost instrumentation, which is available in a limited number of laboratories, all equipped with state-of-the-art high-field NMR spectrometers that provide optimal sensitivity. Still, in 2016 Tee *et al.* reported the detection of hyperpolarized metabolites using a 1T benchtop spectrometer, providing relevant information on pyruvate metabolism in whole cells [86]. Interestingly, they reported longer lifetimes for hyperpolarized substrates at 1T compared to high-field, suggesting that using benchtop NMR in combination with d-DNP could provide a way to better preserve the lifetime of hyperpolarized molecules.

Another practical perspective offered by benchtop NMR in this field is that it provides a convenient way to optimized and develop d-DNP experimental settings without monopolizing a high-field spectrometer. Finally, benchtop NMR could also benefit from the development of emerging transportable hyperpolarization approaches, where the presence of the DNP machine at the point of the NMR detection would ultimately become unnecessary [87]. This would circumvent the current cost and portability limitations of d-DNP, which are rather contradictory with the compact and accessible character of benchtop NMR.

### 5.2. Para-hydrogen induced polarization

PHIP is another very popular hyperpolarization method, based on the naturally high polarization of para hydrogen ($p$-$H_2$) – the singlet-state nuclear spin isomer of $H_2$. In its initial form, PHIP relies on a chemical hydrogenation reaction that is used to place the two $^1H$ nuclei from $p$-$H_2$ in a product molecule, leading to very high NMR signals [88]. This approach has been widely used to characterize the formation of intermediates in hydrogenation reactions [89], or to generate hyperpolarized contrast agents [90]. PHIP remains a relatively selective method since it requires a molecular site that can be hydrogenated. However, a more general approach to PHIP has been developed by Duckett and co-workers, that relies on a reversible exchange of $p$-$H_2$ to the substrate through an iridium catalyst [91]. This method called SABRE (Signal Amplification By Reversible Exchange) makes it possible to hyperpolarize a much broader variety of substrates without the need to hydrogenate them. SABRE has been extensively used in liquid-state applications at high-field, from reaction monitoring [92] to the quantification of metabolites in complex mixtures [93].

Halse and co-workers showed that impressive results could be obtained by applying SABRE hyperpolarization to benchtop NMR (Figure XX). They reported $^1H$ enhancements up to 17,000 for $^1H$ in the case of pyridine. As highlighted by Halse in a recent review, there are several advantages of $p$-$H_2$ hyperpolarization for benchtop NMR spectroscopy [94]. First, it is relatively easy and cheap to generate hyperpolarized substrates through this approach, thus preserving the low cost and accessibility features of benchtop NMR. $p$-$H_2$ gas can be generate off-site, stored from many hours and easily transported. Second, it provides high polarization levels and third, it can be generated continuously, making it an ideal candidate in flow chemistry settings [95]. It also has some drawbacks such as its selective character –not all molecules can be hyperpolarized through this approach – and the anti-phase nature of resulting NMR signals. Still, $p$-$H_2$ hyperpolarization and its SABRE variant have been widely used with benchtop NMR settings. First, as mentioned for d-DNP, benchtop NMR can be seen as a convenient way to optimize $p$-$H_2$ hyperpolarization methods, since it provides easier and *in situ* measurements of hyperpolarization compared to high-field NMR [96]. Second, continuous

hyperpolarization flow setups are particularly promising for the inclusion of hyperpolarization devices under the fume hood, in a combined compact experimental setting together with benchtop NMR. Recently, Lemhkuhl *et al.* developed a 3D-printed membrane reactor providing continuous hyperpolarization of SABRE substrates that were consecutively detected by a benchtop NMR spectrometer [97]. Such work opens numerous perspectives for flow chemistry and reaction monitoring under the fume hood.

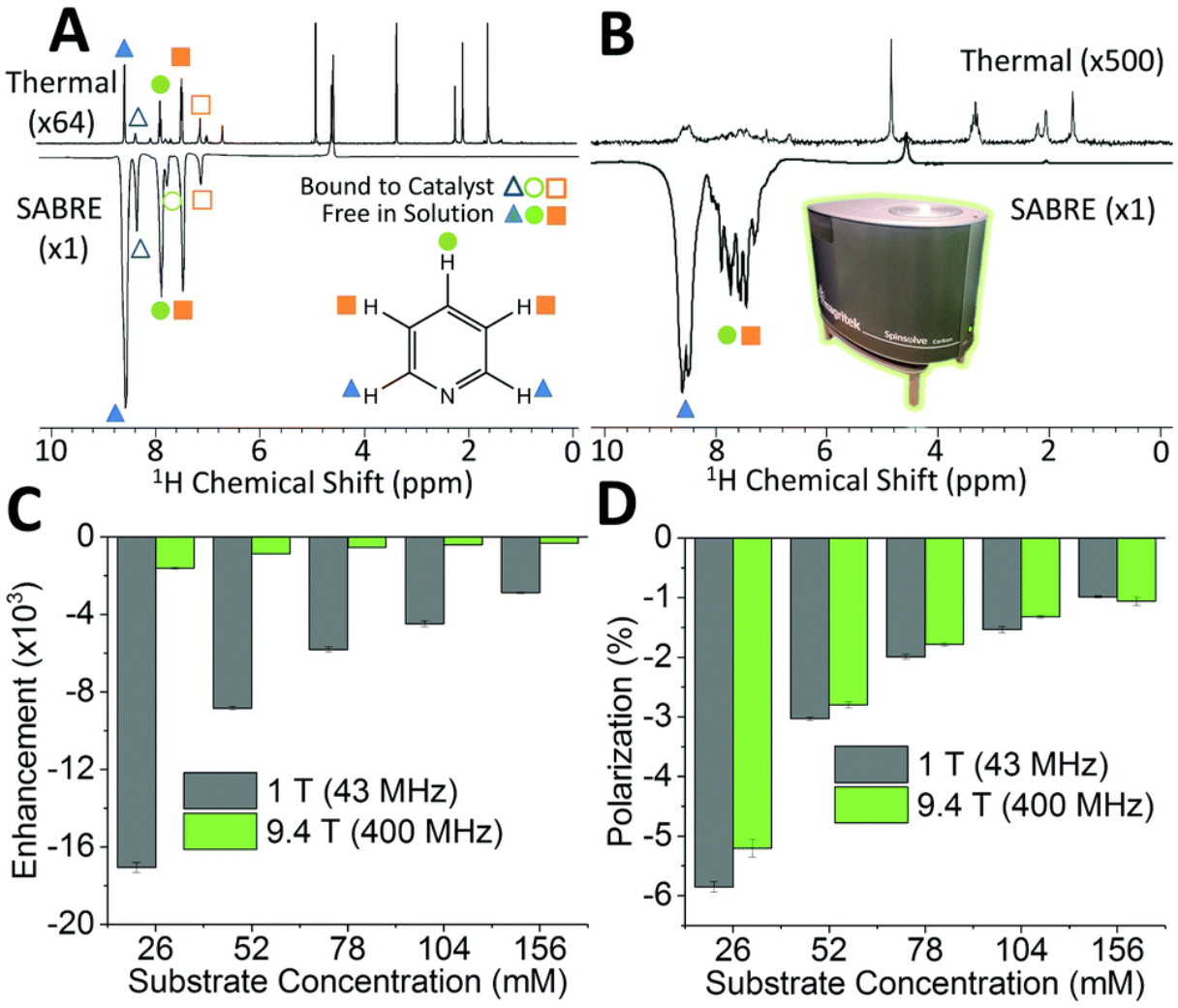


**Figure XX.** Comparison of thermally polarized (top) and SABRE hyperpolarized (bottom) $^{1}$H NMR spectra of 52 mM pyridine with 5.2 mM catalyst in methanol-$d_4$ for NMR detection at (A) 9.4 T and (B) 1 T. (C) SABRE enhancement factor, $\varepsilon$, and (D) polarization level, $P$, for the *ortho* resonance (blue triangle) as a function of substrate concentration with NMR detection at 1 T (gray) and 9.4 T (green). Error bars represent the standard deviation across 5 measurements. Reproduced with permission from Ref. XX.

### 5.3. Applications to reaction monitoring

Benchtop NMR is particularly promising for reaction and process monitoring, as described in Sections 7. Along this line, methods that can improve the sensitivity of the benchtop NMR detection for such applications are particularly promising. Along this line, a few papers were recently published that rely on the online monitoring of reactions involving *p*-$H_2$ hyperpolarized substrates.

In 2018, Jeong *et al.* showed that a PHIP system could be combined with a 60 MHz benchtop NMR spectrometer (Figure 14) [98]. This system was used to monitor in real time the hydrogenation of alkenes mediated by Wilkinson's catalyst. The results obtained under different solvent conditions highlighted mechanistic insights that were in agreement with previous literature, showing the potential of their approach to better characterize and understand mechanistic pathways.

Another recent illustration of the potential of hyperpolarized benchtop NMR to reveal mechanistic information was published by Semenova *et al.* Authors showed that SABRE-enhanced $^1$H NMR spectroscopy could be used to monitor reactivity at mM concentrations in a non-deuterated solvent through the quantification of hyperpolarization lifetimes. They monitored the formation of the SABRE catalyst from a pre-catalyst, providing information on hydrogen isotope exchange within the substrate, 4-aminopyridine. Comparable results were obtained at high-field (9.4 T) versus benchtop (1 T). The example is particularly interesting since at these concentrations, benchtop NMR could not be used without hyperpolarization due to low sensitivity and peak overlap.

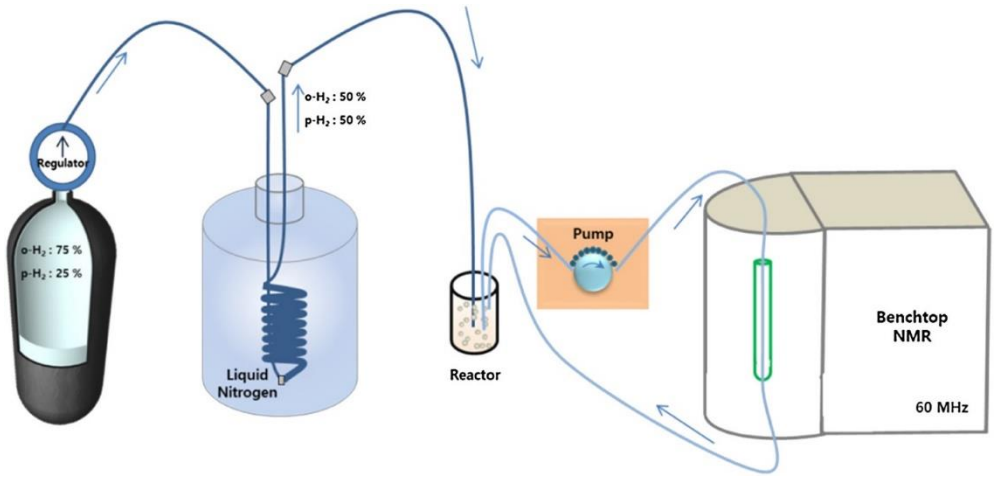

Figure 14. Integrated reaction monitoring system with PHIP and benchtop NMR. 50% hyperpolarized *p*-$H_2$ after passing through the catalyst in liquid $N_2$ is harnessed for the PHIP reaction in the reactor. The reaction mixture is continuously pumped into the benchtop NMR instrument for monitoring.

While hyperpolarization can circumvent the sensitivity of benchtop NMR, such improved sensitivity may lead to increased peak overlap due to the detection of a higher number of species. Therefore, it could be particularly interesting to combine hyperpolarized benchtop NMR with pulse sequence capable of providing improved peak separation while being compatible with flow conditions, such as fast multidimensional NMR methods. Such an achievement was recently published by Gołowicz *et al.*, who combined PHIP hyperpolarization with a fast 2D NMR detection based on time-resolved Non-Uniform Sampling (NUS) [99]. The interleaved acquisition of 1D and fast 2D spectra provided mechanistic insight into the hydrogenation of ethylphenyl propiolate and ethyl 2-butynoate.

### 5.4. Detection of less abundant nuclei

The hyperpolarization of molecules of interest priori to their detection by benchtop NMR can also be an efficient way to probe low-sensitive and less abundant nuclei, that cannot be easily detected by benchtop NMR at natural abundance, unless the samples are highly concentrated. Halse and co-workers published pioneering work along this line, showing how natural abundance 1D and 2D $^{13}C$ signals could be detected thanks to SABRE-based hyperpolarization [100]. They reported enhancements up to 45,000 in the case of pyridine derivatives at natural abundance. The 2D HETCOR spectrum of a natural abundance 4-methylpyridine sample at 260 mM could be detected in only 69 minutes (Figure 15), while *ca*. 300 days of signal averaging would have been necessary to achieve the same SNR without hyperpolarization.

Finally, also worth highlighting is the development of an approach named SABRE-SHEATH (SABRE in SHield Enables Alignment Transfer to Heteronuclei), that was developed to hyperpolarize $^{15}N$ spins through the SABRE method [101]. One of the main advantages of this method is that it delivers hyperpolarized $^{15}N$ spins with extended lifetimes of several minutes. A variety of compounds were hyperpolarized by this approach – either concentrated molecules at natural abundance or labeled diluted molecules – and successfully detected by benchtop NMR spectroscopy [102].

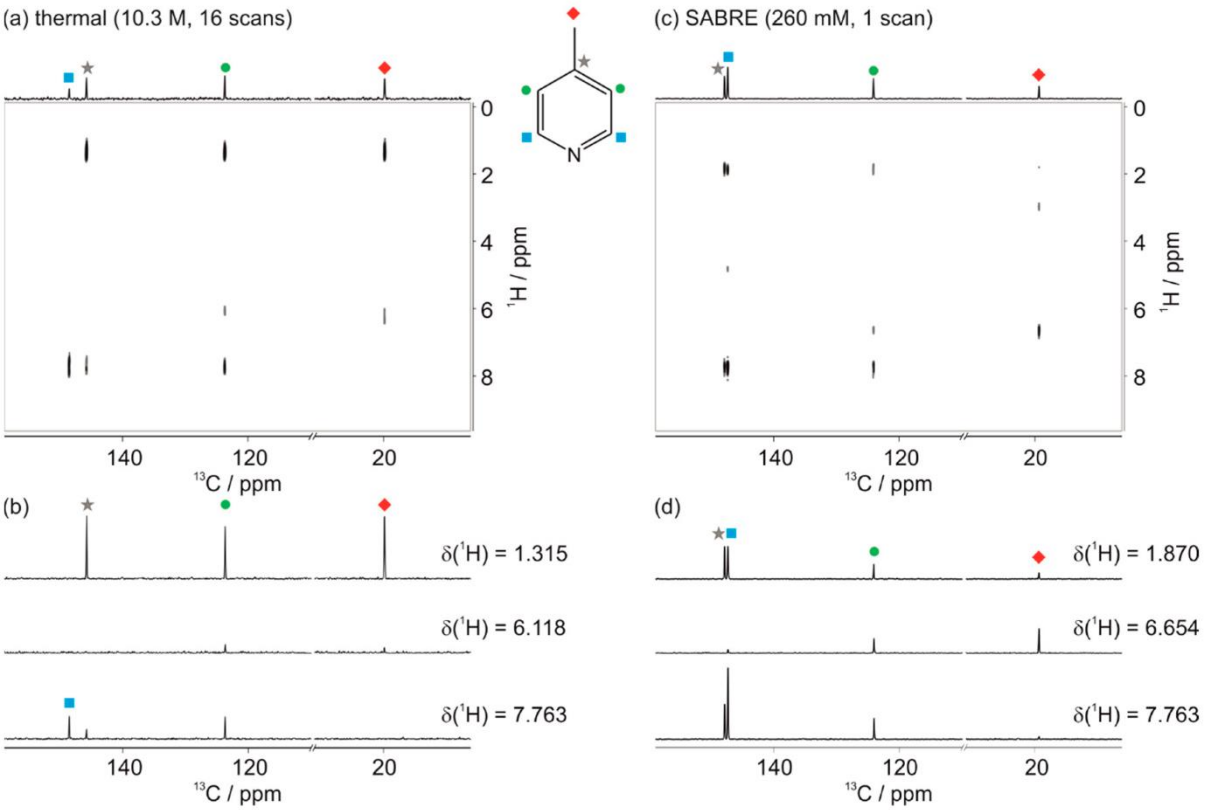


Figure 15. 2D $^{13}C$–$^{1}H$ HETCOR benchtop NMR spectra of 4-methylpyridine (4-MP). (**a**) Thermally polarized spectrum of neat 4-MP (10.3 M) acquired with 64 steps each with 16 scans in a total experiment time of 307 min (5.1 h). (**b**) 1D slices through the 2D spectrum in (**a**) at the chemical shift of the methyl proton resonance (top), meta proton resonance (middle), and ortho proton resonance (bottom). (**c**) SABRE-hyperpolarized 2D spectrum of 260 mM 4-MP with 5.2 mM active SABRE catalyst in methanol-$d_4$ acquired with 90 steps each with a single scan in a total experiment time of 69 min. (**d**) 1D slices through the 2D spectrum in (**c**) as in (**b**). Note, the differences in chemical shifts between the two spectra are due to the presence of the solvent (methanol-$d_4$) in the SABRE case. Reproduced with permission from Ref. XX.

## 6. Advanced processing methods

As described in Section 4, the development of dedicated tailored pulse sequences has made it possible to push the resolution limitations associated with benchtop NMR. Such limitations can also be overcome by advanced processing methods. This is particularly important in the field of industry, where benchtop NMR can be used as a Process Analytical Technology (PAT) requiring a high level of automation. Advanced processing strategies have thus been developed, which include multivariate methods such as Partial Least Square Regression (PLS-R) and Indirect Hard Modeling (IHM). These methods can work efficiently at the condition that spectra are properly phased and baseline corrected, and this also requires a certain level of automation.

### 6.1. Signal processing

Before exploiting spectral data, signal pre-processing steps are crucial to obtain exploitable spectra, including phase and baseline correction. This is not specific to benchtop NMR, but at medium magnetic field, these steps are even more crucial due to the ubiquitous peak overlap and strong coupling effects. Sawall *et al.* developed an algorithm which was particularly suited to medium-field NMR spectral, consisting in simultaneously phasing and baseline correcting the spectrum through a multi-objective optimization (Figure 16). Other methods typically used for high-field spectra could also help solving this issue in the future, such as Entropy minimization [103], Coarse and Fine tuning procedures for 1D and 2D spectra [104] or the Steiglitz-McBride algorithm [105]. ~~are able to automatically correct the phase of signals [106] but also simultaneously with the baseline flattening (Figure 16) [107].~~

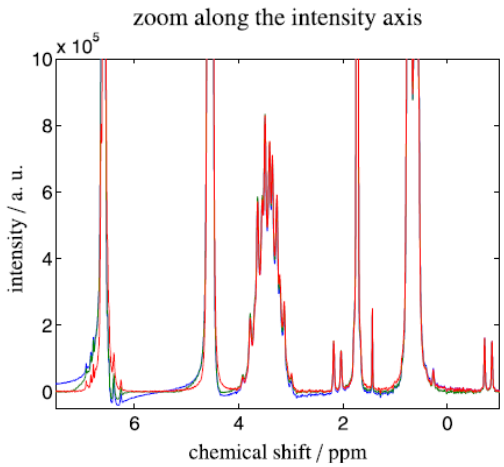


Figure 16. 43 MHz NMR spectra for the binary mixture of 2-propanol and toluene after application of three forms of data preprocessing. Zoom along the ordinate-direction. The blue spectrum results from exclusive application of the phase correction, and the green spectrum is the outcome of a consecutive application of the phase and baseline correction steps. The new simultaneous phase and baseline correction algorithm yields the red spectrum. Obviously the best spectrum results from the simultaneous correction algorithm. (For interpretation of the references to colour in this figure legend, the reader is referred to the web version of this article [107].

### 6.2. Data processing

Once the spectra have been properly phased and baseline corrected, extracting relevant information can be more difficult than at high-field due to ubiquitous peak overlap. Direct line integration and line fitting are widely used at high-field since they do not require any calibration data [108], but their use becomes problematic at medium field. Building robust and predictive reproducible models made of

suitable training data sets can help extracting relevant data from highly overlapped benchtop NMR spectra. In this approach, models are typically built from a set of spectra with a known composition. Data processing methods need to account for speed and accuracy requirements, so that they can be used to control industrial processes with a high level of automation.

A first approach, PLS-R, is well known in the field of near IR spectra analysis [109]. Moreover, multivariate approaches are also commonly utilized at high magnetic field for metabolomics [110]. PLS-R uses a soft linear empirical model being entirely data-driven. The multivariate calibration by regression links NMR spectra (X) to concentrations of the analytes (Y). PLS-R controls data reduction for functionally correlated data by finding components from X that are also appropriate for Y. It seeks for a set of components (called latent vectors) that performs a simultaneous decomposition of X and Y with the constraint that these components explain as much as possible of the covariance between X and Y. Because PLS-R is a linear method, it typically requires additional latent vectors to model nonlinear effects such as peak shifts or deviations of line shape that are typical for NMR spectra. PLS-R allows for the decomposition of the NMR spectra as well as for the quantity of molecules composing the sample under study.

An alternative data processing strategy, IHM, relies on a hard model of pure component spectra. IHM is based on the sum of Gauss-Lorentz or Voigt functions that represent the peak in the pure component spectrum. The model looks like the signals using the Lorentz-Gauss parameters (Figure 17.a) that can be referred to signal chemical shift and couplings as well as concentrations. A model mixture spectrum is built, (Figure 17.c) involving 12 to 21 signals per pure component with known concentrations (Figure 17.b) depending on each system under study. Spectral data (Figure 17.d) are fitted with the model mixture spectrum, and the fitting procedure is based on the minimization of the signal residuals.

While the component weight parameters are linked with the component concentrations, the peak parameters are chosen to describe the spectrum fingerprint. Peak shifting arising from pH, temperature, or susceptibility variations can be considered for within predefined limits. Unlike other

methods, the model is able to extrapolate, as the component weights are robust against peak changes. The creation of the hard model is fully automated, as well as the fitting of mixture spectra.

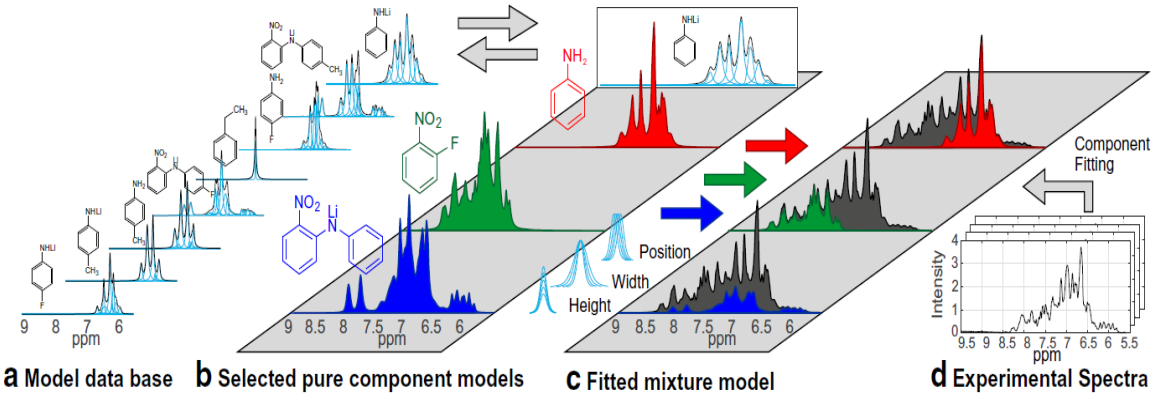


Figure 17. Indirect Hard Modeling (IHM) workflow for quantitative evaluation of measured NMR spectra (d) by building a mixture model (c). Relevant pure component models (b) for each process can be selected from pure a component model database (a) and employed together with model constraints. Cyan, lines represent peak functions of each spectral model. Figure reproduced with permissions from [111].

The two previously described multivariate approaches IHM and PLS-R were recently compared on an industrial lithiation process [111]. Online benchtop NMR data was analyzed by IHM with low calibration effort, compared to a multivariate PLS-R approach, and both methods were validated using online high-field NMR spectroscopy. Maiwald *et al*. further applied this strategy to investigate an esterification reaction with both $^{1}H$ and $^{19}F$ benchtop NMR. Spectra were automatically phased and baseline corrected, then analyzed by both PLS-R and IHM methods.

Both approaches have their own advantages and drawbacks. PLS-R models are built from calibration spectra containing reactants and products with known composition. The calibration samples should cover both the relevant concentration range and the matrix of the expected reaction to provide stable PLS-R models. Changes in reaction conditions such as temperature, pH etc. that may affect line shapes or peak positions should be included at the stage of model building, otherwise, the prediction powers of PLS-R is hampered. In addition, the PLS-R pretreatment – selection of variables and validation method – require a significant amount of work. On the contrary, IHM relies on prior knowledge of reactants and products, *i.e.* the pure component spectra. If only component fractions are derived and

since the signal of the analytical method is directly proportional to the amount of substance, it can likewise be used without calibration. Authors of the above mentioned studies found that IHM was more robust towards changes in experimental conditions. IHM could reduce the user input due to peak fitting of pure component spectra and optimization of peak constraints. Moreover, IHM requires minimal calibration efforts. However, Kern *et al.* reported that it leads to higher Root Mean Square Errors (RMSE).

An alternative method was recently reported for the quantitative analysis of medium-field NMR data, [112]. The model is defined by quantum mechanical parameters of the underlying spin systems and is inherently field-invariant. The accurate values of chemical shifts and J-coupling constants determined from well resolved high-field spectra are used to model data acquired at medium-field strength. The efficiency of this method was illustrated on polysaccharides, which are commonly difficult molecules to analyze due to their short chemical shift range for most of $^{1}$H. Moreover, they are difficult to assign due to their conformational changes. Sugar model mixtures as well as yellow kiwi juice (Figure 18) were used to show the potential of this field invariant technique to retrieve spin systems at medium field and to determine concentrations with a good precision. Quantitative data have been obtained with an error lower than 1% from a 43 MHz, in very good agreement with those obtained at 400 MHz.

More recently PAT monitored on a 43 MHz compact instrument have been combined with extended fast artificial neural networks to predict concentrations in real time on a four component reacting process.

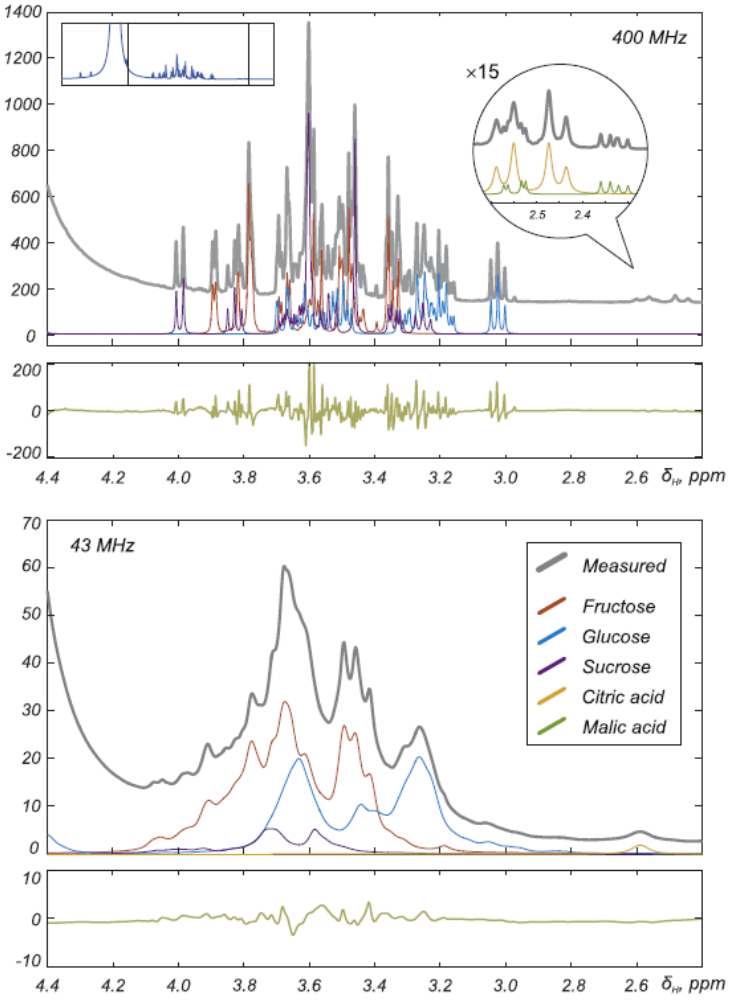


Figure 18. Examples of spectra of a juice (yellow kiwi) acquired at different field strengths along with fitted models of sugars and two acids. The residual signals between the models and the data are shown beneath each graph. Reproduced with permission from [112].

# 7. Applications to reaction and process monitoring

This section is dedicated to reaction and process monitoring, which form the most widely reported application of benchtop NMR. As the size of benchtop spectrometers allow them to hold under a fume hood, the coupling with a reactor is easily performed with common tubing and pumps. NMR is a flow-compatible and non-invasive analytical method, and most organic molecules present several $^{1}H$ sites that can be detected by NMR. Only one well-resolved signal is necessary to monitor the consumption or the production of a given molecule, which is very interesting at medium-field since $^{1}H$ chemical shifts tend to overlap. When peaks are not sufficiently resolved, pulse sequences can be adapted (see section 4), if possible the nucleus can be changed (e.g. $^{19}F$ is a very convenient nucleus for NMR because of its sensitivity and its wide chemical shift range [26]) or processing solutions can be envisaged (see section 6). Finally, in accordance to the quantitative NMR conditions, analyte absolute concentrations can be measured through a single internal reference [113,114], making it relatively straightforward to determine reaction yields.

### 7.1. Monitoring conditions

Different practical approaches can be considered for such reaction monitoring:

- Offline monitoring: a volume of reaction is periodically removed, potentially quenched and then analyzed. This procedure requires human intervention as well as a substantial volume of solution. Actually, the extracted volume can be analyzed with any analytical technique and the relevance of benchtop NMR is limited in this case. To our knowledge, this strategy has never been published using a benchtop spectrometer, certainly for this reason.
- In situ monitoring: reagents are put in the NMR tube inside the spectrometer and spectra are recorded over the course of time. This monitoring strategy presents the advantage of being completely non-invasive (no extraction) in a very small volume of solvent which can be deuterated in order to acquire NMR spectra without one or several overwhelming solvent

peak(s). The main drawback of this monitoring approach is the lack of control of the reaction, especially the lack of stirring. Stirring has a strong effect on reaction kinetics rates, and this feature was well-highlighted by Foley *et al.* [115]. Their kinetic results on the self-condensation of propionaldehyde are shown in Figure 19, showing how the absence of stirring can considerably alter reaction kinetics.

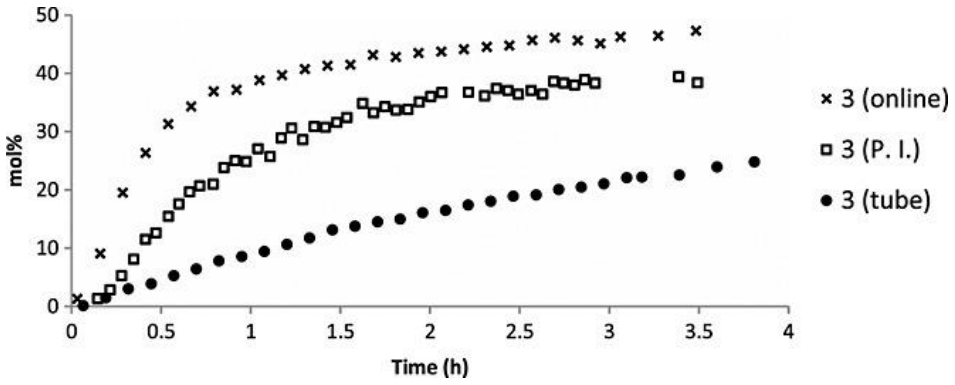


Figure 19. Product formation of the L-proline-catalyzed self-condensation of propionaldehyde. The difference in the reaction kinetics is induced by the three monitoring strategies. The lack of stirring in the monitoring in a tube (full dots) induces a slow reaction. This is partially overcome through a manual mixing of the tube between acquisition (P.I.: periodic inversion, squares). Finally the online monitoring ensure a good stirring and the faster conversion rate (crosses).

- Online/inline monitoring: this is certainly the most widely used approach to monitor reactions by benchtop NMR. The reaction mixture is driven from the reactor to the benchtop spectrometer through tubing with a flow system. The analyzed volume can be driven back to the reactor, forming a bypass loop and keeping the volume constant (online) or driven to a second reactor, a waste, etc. (inline). The simplest setup is a bypass loop, which is usually not controlled in terms of temperature or any necessary feature for the reaction which is only available inside the reactor (e.g. gas bubbling, light exposition, solid support/catalyzer, etc). Consequently, inside the bypass section the reaction can be delayed or even cancelled. This is why tubing should be as short as possible to minimize the residence time outside of the reactor. For this reason, benchtop NMR spectrometers are more favorable than their superconducting counterparts for online monitoring, since high-field magnets require longer tubing. Singh *et al.* [116] reported multiple monitoring of an acetalization reaction in order to

investigate several parameters on the reaction kinetics. They also compared the monitoring of this reaction by online benchtop NMR (43 MHz) with offline high-field NMR (400 MHz) and gas chromatography, shown in Figure 20.

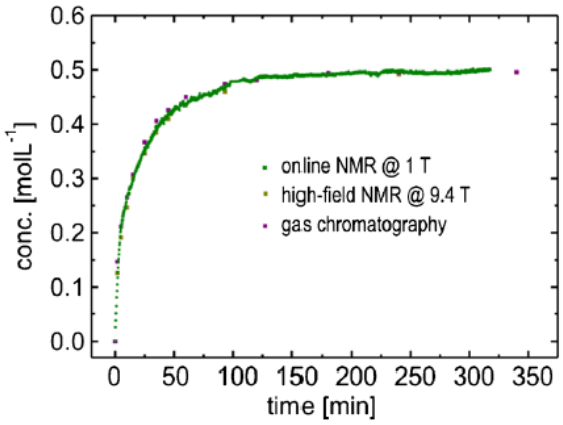


Figure 20. Comparison of an acetalization reaction monitoring: by online benchtop NMR (43 MHz), offline high-field NMR (400 MHz) and gas chromatography.

Reaction kinetics were found extremely similar for the three approaches. However, benchtop NMR has the advantages of providing more kinetic points, is much less human-time consuming and is cheaper than the other techniques. These reasons make benchtop NMR a relevant and accessible device for monitoring purposes. A last advantage of performing NMR in flow conditions consists in taking advantage from the "inflow effect" [32]. Indeed, during the repetition time of the experiment, the flow brings freshly non-excited polarized spins within the sensitive volume. Properly exploited, this effect allows to accumulate NMR scans at a higher rate than in static conditions and so increase the sensitivity over time [117].

### 7.2. NMR strategies

The broad variety of NMR pulse sequences that have become available on benchtop spectrometers also helped broadening their potential applications to monitoring. Two families of pulse sequences are particularly relevant for flow conditions and reaction monitoring:

- Signal suppression pulse sequences for saturating the solvent peak(s) that may cover pertinent regions of the NMR spectra as well as induce dynamic range issue [32]. For example Soyler *et*

*al.* [118] reported the online monitoring of the sucrose hydrolysis. Although they were close to the water peak, sucrose and free glucose proton signals were well-resolved and could be efficiently integrated for the reaction monitoring, thanks to the use of the WET-180-NOESY pulse sequence [32].

- UF pulse sequences which can record multidimensional spectra in a single scan [69,73]. Indeed, the classical way of acquiring multidimensional spectra suffers from the evolution of the sample during the reconstruction of the indirect dimension and can lead to spectral distortions. The suitability of using an ultrafast pulse sequence for reaction monitoring was reported by Gouilleux *et al.* [73]. The authors monitored a Heck-Matsuda reaction in a tube with a UF COSY pulse sequence (Figure 21). This approach was further applied under flow conditions [34], showing as expected a significant acceleration of reaction rates upon stirring.

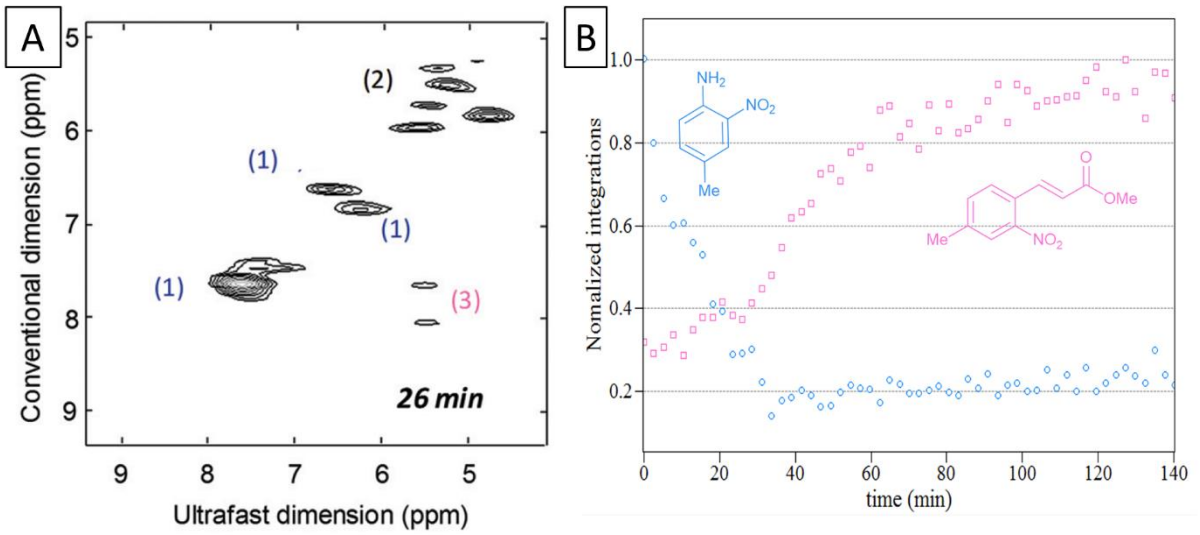


Figure 21. Monitoring in a tube of a Pd-catalyzed Heck-Matsuda reaction by benchtop NMR spectroscopy (43 MHz) through the UF COSY pulse sequence. A is one $^{1}$H-$^{1}$H UF COSY spectrum at 26 minutes of reaction in the middle of the reaction where both reactant (blue) and product (pink) peaks are visible and labelled. B compiles the reactant and product monitoring curves over time. Adapted with permissions from [32].

In addition to these pulse sequence strategies, hyperpolarization methods (Section 5) are also expected to significantly impact reaction monitoring. Gołowicz *et al.* reported an impressive combination of hyperpolarization with pulse sequences, applied to online monitoring [99]. Cleverly combined a para-hydrogen flow setup (Figure 22.A) with 2D Double Quantum Filter (DQF) COSY pulse

sequences accelerated by NUS (Figure 22.B). The authors managed to observe the hydrogenation, enhanced by the $H_2$ hyperpolarization, of ethylphenyl propiolate to (Z)-ethyl cinnamate and ethyl 2-butynoate to (Z)-ethyl crotonate.

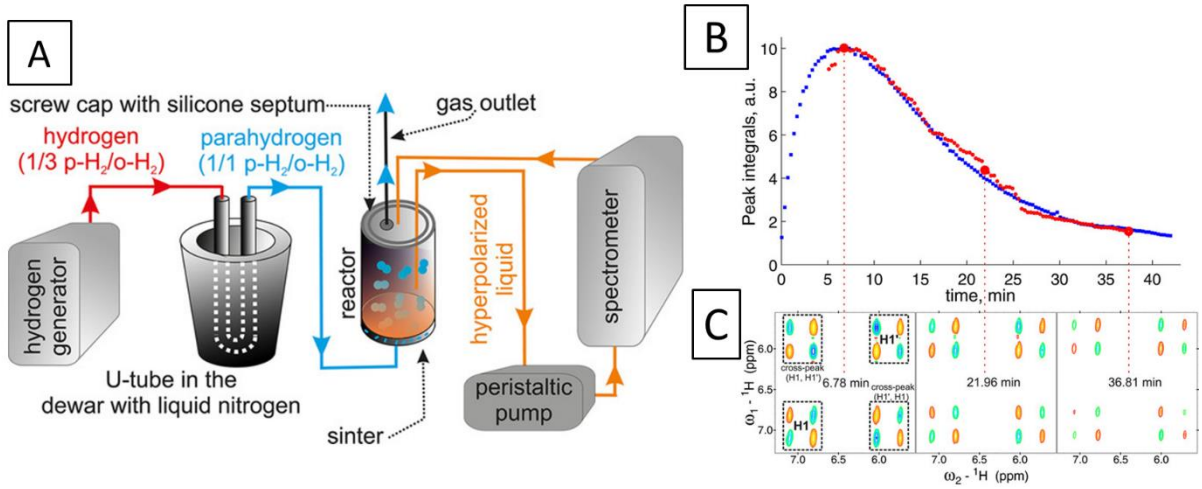


Figure 22. Online monitoring of a hydrogenation reaction with benchtop NMR (43 MHz) enhanced signal by para-hydrogen flow setup. A: scheme of the flow setup using a enriched para-hydrogen gas bubbling in the reactor. The benchtop NMR is connected to the reactor by a bypass loop. B: monitoring of the (Z)-ethyl cinnamate signal through interleaved $^1$H (blue) and $^1$H-$^1$H DQF-COSY (red) pulse sequences. The use of hyperpolarized $H_2$ enhanced the freshly-formed product signals and so the signal rapidly reaches a maximum when the hydrogenation rate is maximum, quickly after (ca. 5 min) the injection of $H_2$. The hyperpolarized effect rapidly vanishes, the product signal decreases since there are less and less freshly-formed product. C: Overview of three $^1$H-$^1$H DQF-COSY spectra at 3 different times of the reaction.

### 7.3. Integration in complex flow setup

Thanks to their ability to provide quantitative results, benchtop NMR spectrometers were successfully used in several articles dealing with flow chemistry [56,119] in which they can easily provide reaction yields. Benchtop NMR can also be considered as an analyzer in downstream of a liquid-state separation technique. This application has been reported in the article of Botha *et al.* [57] in which they used inline NMR spectroscopy as a detector of a Size Exclusion Chromatography (SEC). By combining the size discrimination of SEC and the chemical shift information, authors were able to differentiate two polymers with identical retention times and different chemical shifts.

Benchtop NMR spectroscopy can also be part of more complex flow setups. The integration of benchtop NMR spectrometers in processes has been reported, often as proof-of-concepts before being part of industrial large-scale processes [120–122]. As mentioned in section 6, Kern *et al.* were

able to perform the inline monitoring of an industrial lithiation reaction [111]. The scheme of the process is shown in Figure 23 in which benchtop NMR continuously analyzed the stream product. The resolution of their benchtop spectrometer (43 MHz) did not provide isolated signals for the involved compounds and multivariate processing was thus used to extract the information (details given in Section 6). By correlating benchtop NMR spectra to high-field NMR spectra (500 MHz) data, they managed to build models for the prediction of the monitoring of the aniline (reactant), the 1-fluoro-2-nitrobenzene (reactant) and 2-nitrodiphenylamine (product).

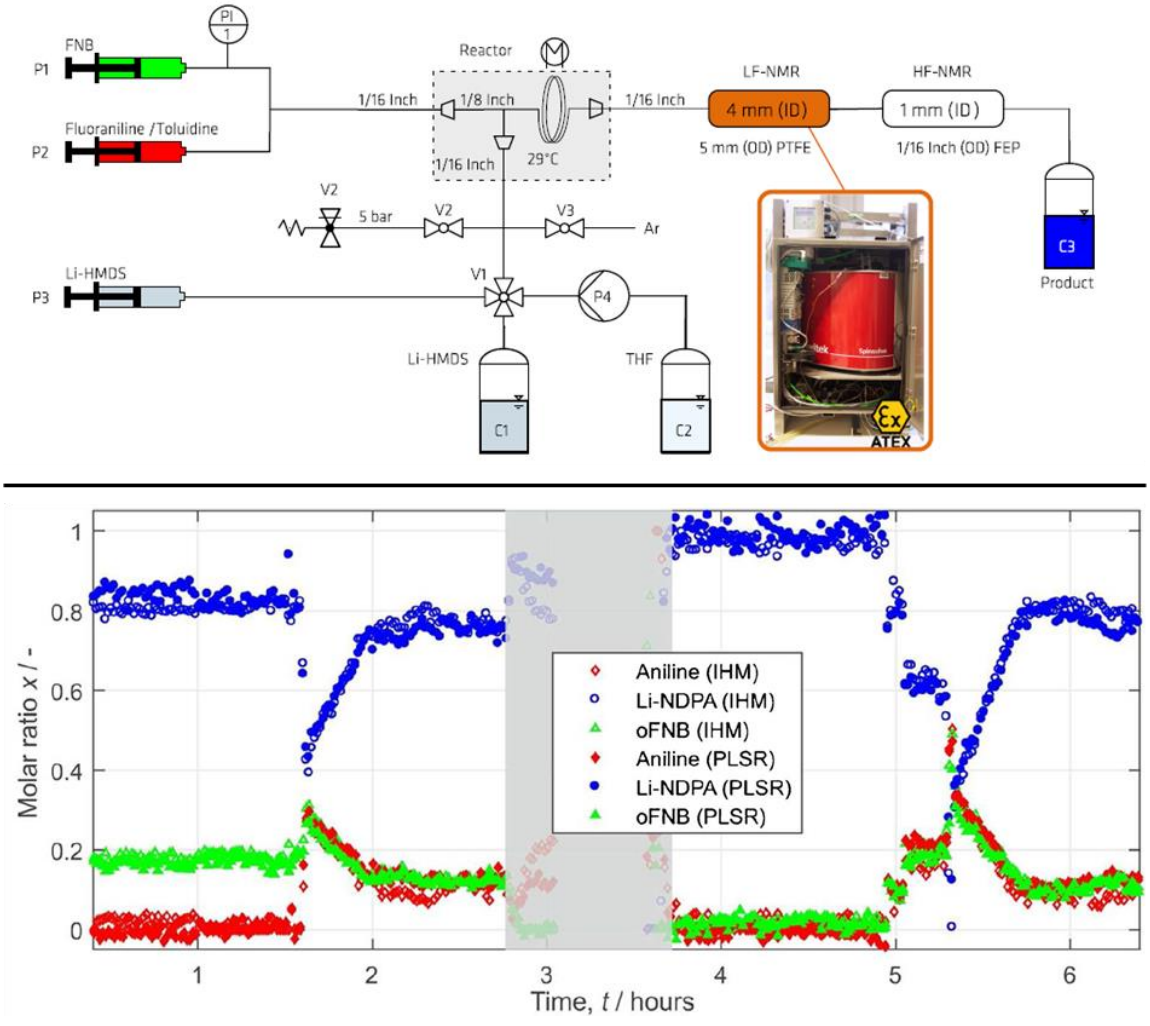


Figure 23. Inline monitoring of an industrial lithiation reaction. Scheme of the set-up (top) and predicted monitoring curves (bottom) of the analine, the 1-fluoro-2-nitrobenzene (oFNB) and the lithium 2-nitrodiphenylamine (Li-NDPA). Two different multivariate processing were used corresponding to the full and empty marks in the graph.

Real-time process monitoring also provides interesting options to control reaction parameters, for instance to determine the optimal moment when a reactant should be added or a parameter modified.

Such process control could even be completely automatized through intelligent algorithms. This requires to automatize both data acquisition and processing steps and to link the resulting data to an operation of the process. Flow chemistry has laid the first stone in developing self-automatizing machines for reaction optimization. Sans *et al.* [119] demonstrated the implementation of a feedback algorithm based on NMR spectroscopy data to optimize an imine synthesis. The reaction was repeated in varying the parameters (molar fraction in reactant, residence time in reactor). The yield was then calculated from the resulting $^{1}$H NMR spectrum. The algorithm analyzed successive NMR spectra to tune the reaction parameters in order to obtain the best yield with the highest concentration of the starting aldehyde and with the minimum residence time. Such feedback algorithm was also used in a study by Cortés-Borda *et al.* [123] for the self-optimization of crucial reaction steps in the production of carpanone. Inline benchtop spectroscopy was used to determine the reaction yield, the latter being used in a feedback loop with optimized algorithms to adapt the reaction conditions, resulting in an intelligent flow chemistry setting (Figure 24). Such approaches based on benchtop NMR are at their early stage but would certainly be an asset for the future of process industry.

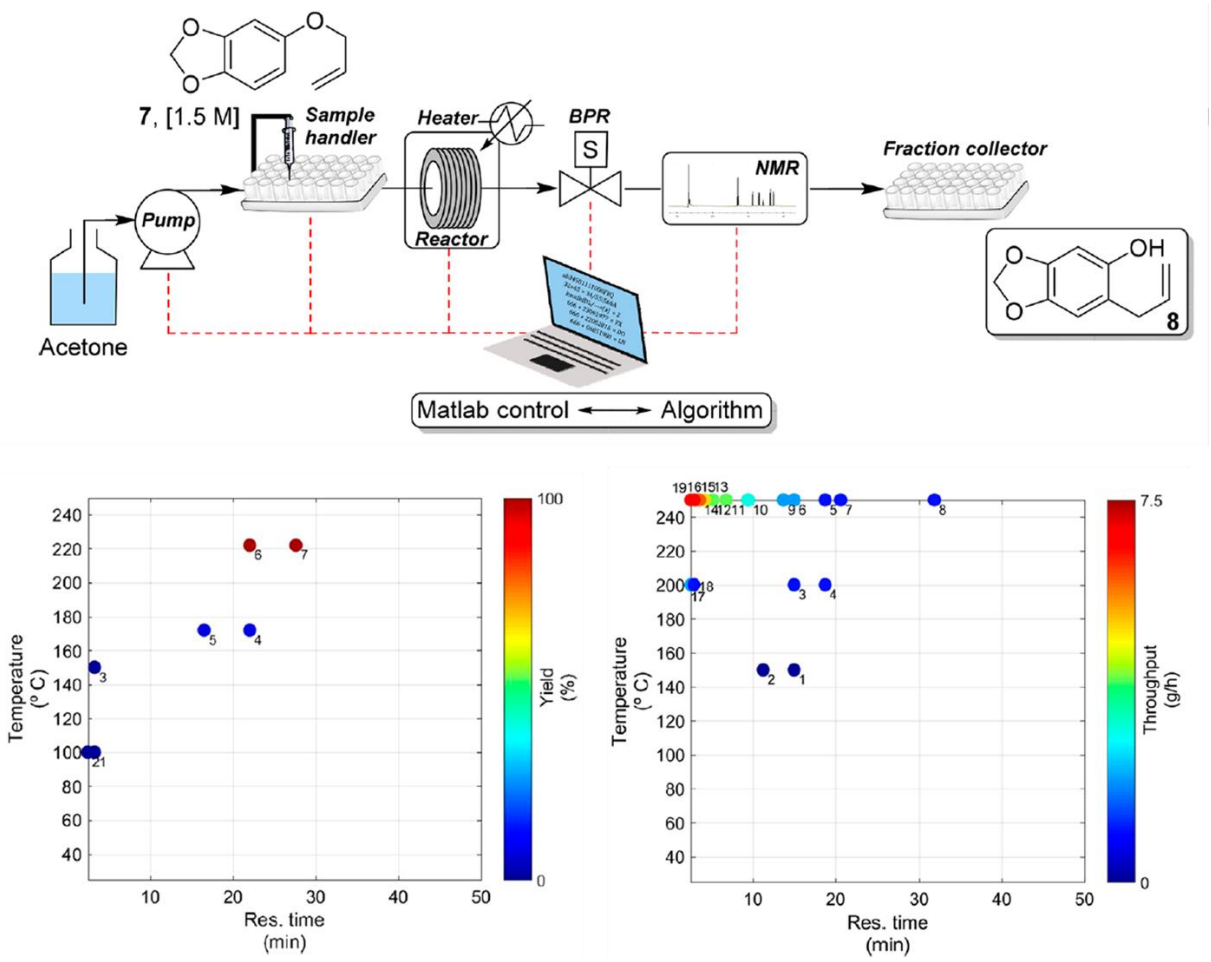


Figure 24. Setup of the self-optimizing process of the product 8. The algorithm changes and optimize the temperature and the residence time in the reactor. Graphs represent the contribution of the two reaction parameters on the yield or on the productivity.

### 7.4. Bioprocess monitoring

Benchtop NMR spectroscopy has also showed great potential for the monitoring of bioprocesses. Bioprocesses involve living organisms to perform operations such as fermentation. Consequently, bioprocesses usually involve suspended biomass which is detrimental to the quality of NMR spectra. In particular, the sample inhomogeneity may lead to dramatic losses in magnetic field homogeneity which affects the lineshapes, resulting into broader NMR signals. However, performed on reasonably concentrated sample, the slight broadening of NMR peaks does not prevent the detection of relevant peaks, as highlighted by the study of Kreyenschulte *et al.* [124] who monitored fermentation processes through online benchtop spectroscopy. The setup scheme and the monitoring curves are shown in Figure 25, demonstrating the ability of benchtop NMR to monitor extracellular compounds in a

suspension medium by a very simple setup. Simultaneously, the alkyl protons of intracellular lipids also gave rise of a NMR signal and their concentration could be monitored. All the monitored concentrations were successfully correlated to an offline technique.

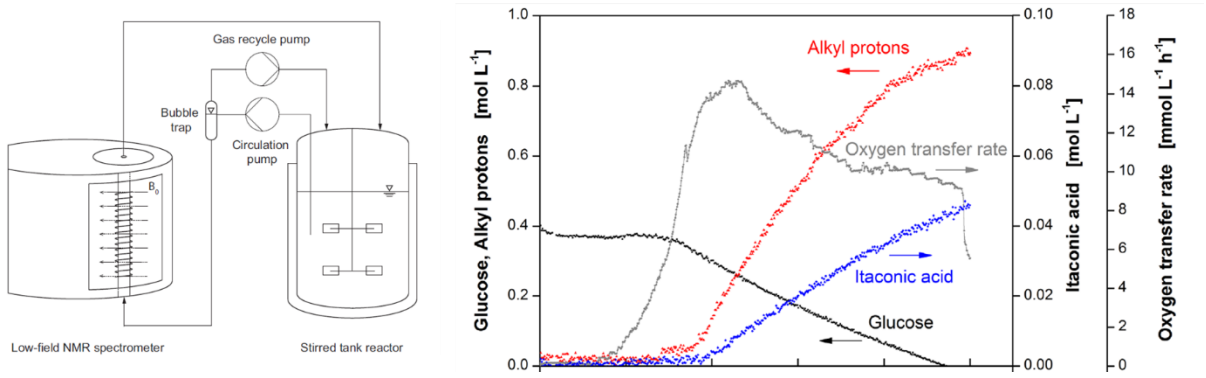


Figure 25. Online monitoring of *Ustilago maydis* fermentation process through benchtop NMR (43 MHz) spectroscopy. The consumption of glucose and the production of itaconic acid are known in real-time. Intracellular lipid protons are also detectable and their concentration can be monitored. Adapted with permissions from [124].

Analyzing intracellular compounds in a non-invasive fashion is not easily performed with other analytical techniques. In this field, Bouillaud *et al.* [125] developed an innovative approach to monitor intracellular lipids by studying, through benchtop NMR, the accumulation of intracellular lipids in microalgae bioprocess (*Parachlorella Kessleri*). After the implementation of an appropriate water suppression pulse sequence (see section 4), the water peak SNR was reduced by a factor of 27,000, allowing to detect weak intracellular lipid peaks (Figure 26). Intracellular lipids were monitored through the $CH_2$ lipid signal. Data were coherent with an off-line reference technique (fatty acid methyl ester analysis by gas chromatography). It should be noted that no other analytical techniques were reported to monitor intracellular lipids without high biomass concentration and significant multivariate processing. Therefore, benchtop NMR spectroscopy opens relevant perspectives in the domain of bioprocesses. As suggested above for chemical processes, the integration of benchtop NMR data to feedback algorithm could be a game-changer for bioprocesses condition optimization. Finally, the incoming developments of spectrometer hardware, especially the increase of the magnetic field strength, will make the technology more and more sensitive and resolved, allowing to monitor more analytes at lower concentrations.

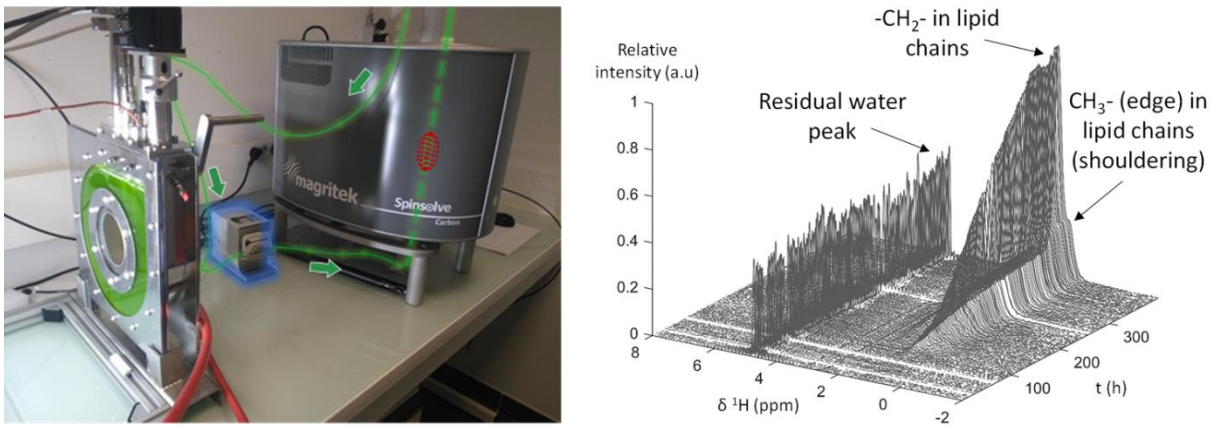


Figure 26. Online monitoring of microalgae bioprocess by benchtop NMR spectroscopy (43 MHz). A simple bypass loop connect the photobioreactor with the benchtop NMR. The resulting $^{1}H$ spectra are recorded with a water suppression pulse sequence (W5) and highlights the accumulation of intracellular lipids over the course of the time.

# 8. Applications to quality control and profiling

Apart from reaction and process monitoring, the second area where benchtop NMR is widely used is the quality control of complex samples through profiling approaches. Such approach has found applications in food science, but also in forensics and pharmaceutical sciences, with promising recent perspectives in clinical metabolomics.

## 8.1. Quality control in food science

Low magnetic field NMR has been used for decades in food science through relaxometry, which explains why benchtop NMR spectroscopy has easily found applications in this field. In particular, it has been used to detect the adulteration of vegetable oils, whose purity and authenticity have been long-standing concerns. Indeed, the international demand is increasing, resulting in common adulteration procedures that consist in adding cheap oils in a high priced oil, this adulteration is a major problem for consumers who find themselves paying a very high price for a cheap oil. NMR offers an interesting alternative to chromatographic methods, since it requires simplified sample preparation and data analysis. Benchtop NMR is particularly promising in this area owing to its low cost and compact nature.

Olive oil is an illustrative example, since its price can vary from a few euros to a few dozen euros per liter. The first study in this field was performed by Riegel *et al.* who studied the adulteration of olive oil by soybean oil [126]. These two oils are relatively different since olive oil is mainly composed of monounsaturated fatty acids and a small amount of polyunsaturated, whereas soybean oil contains between 50 and 60% polyunsaturated fatty acids, with linoleic acid being the main component. Therefore, it becomes quite easy to differentiate between olive oil adulterated with soybean oil since it will present a much more intense bis-allylic region (2.5-3 ppm). An investigation was carried out on olive oil solutions in $CDCl_3$ in which a quantity of between 0 and 60 %v/v of olive oil was incorporated. Measurements were carried out on a 60 MHz spectrometer, thus presenting a low resolution, but making it possible to differentiate the different classes of fatty acids. A simple integration of the bis-allylic proton signals relative to total of integration of the different compounds allowed to plot a calibration curve to determine the percentage of added soybean oil. A second study was conducted on the addition of hazelnut oil [127]. Twenty extra virgin olive oils and ten hazelnut oils were purchased from various UK retailers in two chronologically separated batches. Mixtures were prepared by combining varying amounts of hazelnut and olive oils, in which the hazelnut oil component simulated an adulterant in the olive oil. In this paper, 144 mixtures of olive oil and hazelnut were made and analyzed using a benchtop spectrometer operating at 60 MHz. A multivariate chemometric approach allowed to differentiate the two oil groups thanks to their NMR spectra. The separation was attributed to the much more intense olefinic region (5-5.5 ppm) for hazelnut oils compared to olive oils (Figure 27), and results suggested that a simple peak ratio could be sufficient to separate the two groups of oils.

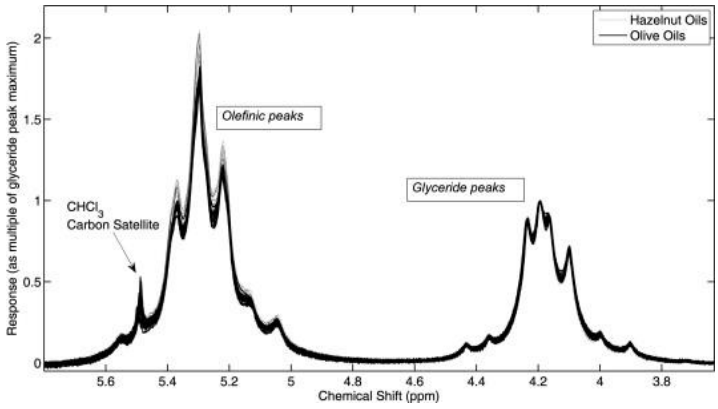


Figure 27. Expansion of the olefinic and glyceride region (3.6–5.8 ppm) for 60 MHz 1H NMR spectra of the pure olive and pure hazelnut oils only. The spectra have been aligned and the spectral intensity scaled to the glyceride peak maximum. Hazelnut oil gives increased olefinic peak intensities. Reproduced with permission from [127]

Other edible oils were also studied by benchtop NMR, such as perilla oil that is also prone to adulteration by soybean oil [128]. $^{1}$H NMR spectra recorded at 43 MHz allowed to discriminate between the authentic and adulterated oil above a 6% adulteration threshold. A more challenging case was tackled by McDowell *et al.* who studied mixtures of Refined Rapeseed Oil (RRO) and Cold Pressed Rapeseed Oil (CPRO) [129]. These oils are very similar in terms of fatty acid composition, most of the variation between these two oils comes from the unsaponifiable fraction which remains in the oils after either cold pressing or industrial extraction. Moreover, SunFlower Oil (SRO) can be an additional candidate for adultering CPRO. By integrating the spectra of 90 binary mixtures of CPRO and RRO or CPRO and processing them with PLS-R, the authors showed that SRO adulteration could be easily detected above a 12% threshold (versus 8% at high field), while RRO adulteration was difficult to detect, both at high and medium field.

While most oil adulteration studies rely on 1D proton NMR, Gouilleux *et al.* suggested to boost the approach by relying on pulse sequences that can better separate overlapped resonances, such as ultrafast 2D COSY [13]. The classification of vegetable oils from 6 different botanical origins was achieved by PCA analysis. 1D proton NMR was compared to UF COSY at 43 MHz with the same experiment time per spectrum (2.4 min). The authors showed that UF 2D NMR provided a much better group separation than 1D NMR on a PCA plot (Figure 28), which could be attributed to the reduced

peak overlap. A PLS calibration model was used to predict the levels of adulteration on olive oil by hazelnut oil.

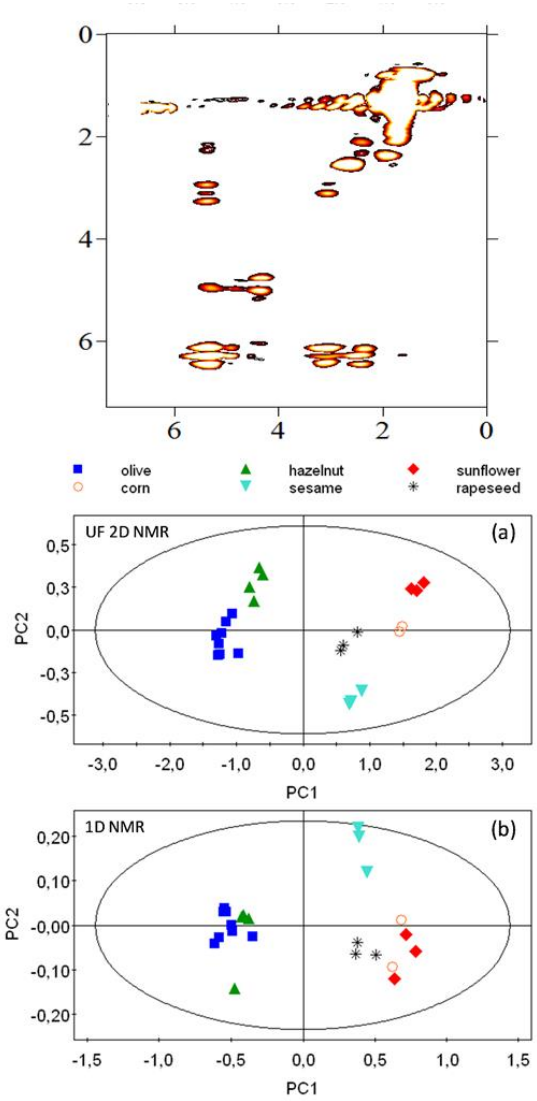


Figure 28. Illustration of the potential of 2D experiments for the profiling of food samples with benchtop NMR spectroscopy. (Top) Ultrafast 2D COSY spectrum recorded in 2.4 min on a sunflower oil sample in non-deuterated chloroform. (Middle) PCA analysis obtained with such UF 2D NMR experiments on 23 edible oil samples from different botanical origins. (Bottom) PCA on the same sample set with standard 1D experiments and a variable bucketing approach. Reproduced with permission from [13].

Apart from oils, other categories of food products are likely to be adulterated. Jakes *and al.* decided to create a method to differentiate horse versus beef meat based upon comparison of tryglyceride profiles using a benchtop NMR spectrometer [130]. The two groups of meats were analyzed in two different laboratories, and were well separated on PCA plots obtained from both benchtop datasets. In another study, Gunning *et al.* showed that the adulteration of more expensive Arabica coffee by

cheap Robusta could be detected by benchtop NMR [131]. Complementary high-field NMR and MS analysis were necessary to show that 16-Omethylcafestol was an indicator of the presence of Robusta beans in the sample. The limit of detection of Robusta in Arabica was estimated to 10-20 %w/w for benchtop NMR while it is valued at 1-3 %w/w for acquisitions at high magnetic field [132].

### 8.2. Quality control in other fields of industry

While benchtop NMR in industry has been mainly used for food science applications, it also offers great promises in other areas of industry. By being compatible with the demanding environment of production lines, benchtop NMR can be a convenient tool for the quality control of end products. For example, Singh and Blümich reported the development of a model to evaluate the quality and homogeneity of raw rubber from benchtop NMR spectra [133]. Styrene-butadiene rubber (SBR) – composed of 4 different units: styrene, vinyl, trans and cis 1,4-butadiene– was studied at 1T through $^{1}H$ and $^{13}C$ acquisitions. Styrene and vinyl were identified by 1H NMR while cis and trans butadiene were identified by $^{13}C$ NMR. Partial least-squares regression in combination with 1D $^{1}H$ was used to quantify the styrene, 1,2-butadiene and 1.4 butadiene units that formed SBR. PLS-R models were generated from 32 $^{1}H$ LF spectra of different SBR, then tested with 15 others spectra for which the concentration of SBR was known. Standard deviations as good as 1-2% were reported, opening interesting application perspectives of benchtop NMR in tire industry.

### 8.3. Pharmaceutical sciences and forensics

Benchtop NMR has been widely used for the profiling and control of pharmaceutical and illegal substances. One of the simplest methods is to qualitatively study the NMR data obtained. For this purpose, the most obvious approach is to rely on databases to identify the structure of known compounds [43]. In some cases, a complete structural elucidation can also be carried out [12]. Resulting spectra can also be used to quantify the active pharmaceutical compounds in a drug, to make sure it has not been falsified or deliberately mislabeled. For example, studies have been conducted on food supplements and sexual enhancement drugs [43] with both high- and medium-field NMR

spectrometers to allow a comparison of the accuracy and precision of the quantification. Analysis showed that almost all formulations were falsified, and that adulterant could be detected in *ca.* 20 min at 60 MHz after a rapid sample preparation. Quantification with an internal standard showed a good accuracy (better than 10%) in that study. In another study, the same authors also analyze medicines for erectile dysfunction and for the treatment of malaria [12]. A qualitative analysis revealed that many samples contained APIs that were not indicated on the packaging or were different from those claimed. The amounts of falsified products could be accurately determined with a detection threshold as low as 0.2 mg of active compound for a 100 mg tablet. This shows that benchtop NMR has the ability to detect drugs which have been deliberately falsified with a small percentage in order to be able to pass the field tests. A complementary quantification approach for pharmaceutical compounds was also demonstrated in an educational context [134]. The study aimed at measuring the ratio of active products in over-the-counter drugs. It began with measurements on pure compounds by students. Then, proportion of compounds in home-made and commercial samples was determined by a simple integration ratio between the different compounds in the sample. The results mentioned in these studies anticipate that benchtop NMR spectrometers could be used in governmental agencies, in the field of pharmaceutical fraud detection.

Recently, benchtop NMR was also used in the field of forensics and more particularly for the characterization of New Psychoactive Substances (NPS). NPS are molecules derived from legal and commercial drugs which have been misused or whose structure has been slightly modified. As a consequence of these chemical modifications, these toxic and carcinogenic compounds are not controlled under the International Drug Control Conventions, and their legal status is not defined. The growing occurrence of these molecules on the European market is an alarming threat for public health because they are widely consumed during festive events as recreational drugs and their use could lead to death by overdose. In this context, there is an urgent need to regulate NPS, and the accessibility of benchtop NMR is particularly appealing to law enforcement agencies. In this context, Assemat *et al.* showed that benchtop NMR could be used to identify and quantify mixtures of NPS present in herbal

spices rom custom seizures [135]. Although peaks were highly overlapped, spectra provided valuable clues on the chemical structures of synthetic cannabinoids with the detection of characteristic signals. Still, full structural elucidation was not possible, highlighting the limitations of benchtop NMR. The authors suggested that this limitation could be partially circumvented by relying on a complementary set of 2D acquisitions.

Alternatively, molecular databases could offer an efficient way to circumvent spectral resolution issues that prevent the use of benchtop NMR to elucidate the structure of NPS. A convincing example relates to the development of an automated algorithm for spectral recognition of NPS [136]. NMR spectra of compounds were collected using an 80 MHz instrument. The reference library consisted of 302 spectra altogether for different classes of NPS. Then, 432 seized samples were analyzed by GC-MS and NMR for cross validation. $^{1}$H NMR analysis nicely matched the GC−MS results for 93% of the seizures. This example highlights the relevance of combining benchtop NMR with databases, and such combination could be made even more efficient when databases contain high field NMR data. Capitalizing on such a strategy, Zhong *et al.* 12 drugs and their derivatives were analyzed by high field NMR to create a library [137]. Subsequently, two samples from seizures were analyzed by a benchtop NMR operating at 80 MHz and compared to high field spectra. This allowed the identification of morphine and acetylcodeine for MMA and MDMA, respectively (Figure 29).

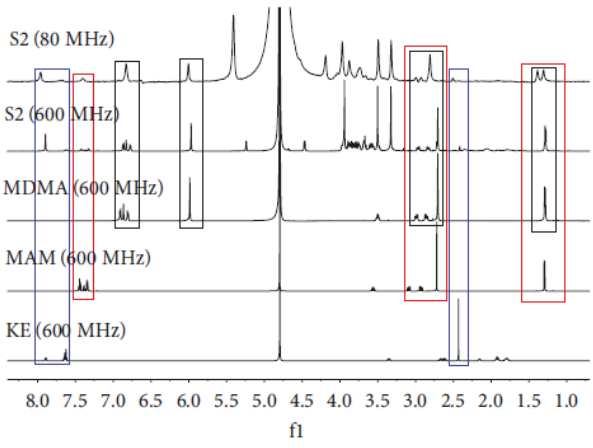


Figure 29. The 1H NMR spectra for S2, MDMA, MAM, and KE. Reproduced with permission from [137]

The above-mentioned examples highlight the capabilities of benchtop NMR as a qualitative method for the analysis of drugs. They also shed light on their limitations in terms of structure elucidation, and on the potential usefulness of databases that can be used regardless of the magnetic field. To facilitate the comparison between high-field and medium-field databases, a technique called Quantum Mechanical Spectral Analysis (QMSA) was recently suggested [138], which makes it possible to transform a spectrum obtained at a high magnetic field into a spectrum obtained at another magnetic field. This could push towards a more general joint use of benchtop NMR and databases in forensic laboratories.

### 8.4. Metabolomics

Metabolomics, or metabolic profiling, is the systematic study of the unique chemical imprint left by biological processes during metabolism. NMR is one of the two major analytical tools in metabolomics, and NMR metabolic profiling has been constantly evolving in the last two decades thanks to numerous methodological developments [139]. The typical NMR metabolomics workflow require high field spectrometers (*eg.* 600 MHz), with high-field spectra being analyzed through statistical approaches to highlight biomarkers of a specific conditions. However, the cost and complexity of high-field NMR equipment has limited the use of NMR in hospitals, contrary to mass spectrometers which are more widely used in a clinical context. Benchtop NMR could possibly play a significant role here, certainly not to elucidate the structure of a new biomarker, but rather when considering untargeted approaches which aim at separating sample groups for classification purposes such as diagnosis. With such fingerprinting strategies, bucketing of the $^{1}$H NMR medium-field spectra could provide sufficient information for group separation. This is particularly the case when sample amounts are not too limited, and the food authentication examples mentioned above already pertain to such “omics” approaches. In the clinical world, benchtop NMR entered the field of metabolomics in 2015 with a study on diabete biomarkers [140]. A first trial was conducted at 60 MHz on 24 patients, including 10 with type 2 diabetes and 14 healthy patients. A typical metabolomics workflow was applied, and PCA analysis made it possible to differentiate between healthy and diabetic patients (Figure 30). Further

statistical analysis was used to determine the biomarkers allowing discrimination between the two groups. The results showed that methylsuccinate (upregulated) and formate (downregulated) were put forward as biomarkers of group discrimination, as well as other markers such as glucose, acetone, 3-D-hydroxybutyrate, acetate, N-acetyl storage compounds, citrate, creatinine and lactate. In addition, the authors showed that urinary glucose levels could be quantified through the signal of α-glucose at 5.25 ppm. Quantitative results were very similar to those obtained at high field. Beyond this example, the potential applications of benchtop NMR could be used for the rapid diagnosis of a large number of diseases, relying on biofluids such as urine, blood or saliva.

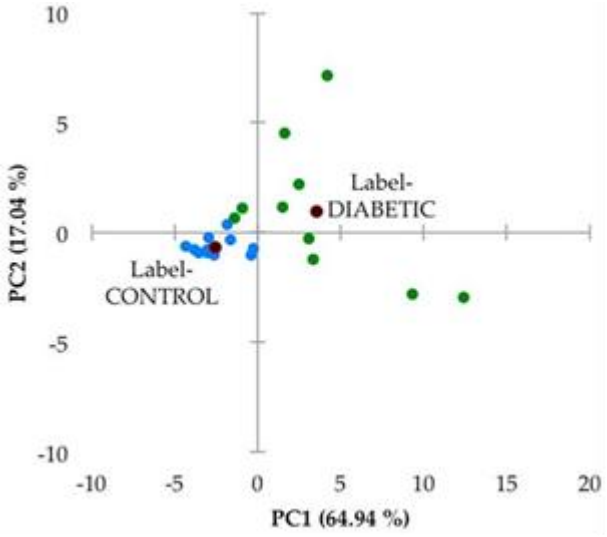


Figure 30. Principal component analysis (PCA) scores plot of PC2 (17.04% of total variance) versus PC1 (64.94% of total variance) for a preliminary investigation of distinctions between healthy control and type 2 diabetic cohorts, and also potential sample outliers. Color codings: blue, urine samples collected from healthy controls; green, those from type 2 diabetes participants. The black points represent scores plot centroids for the two groups explored. PCA was performed using XLSTAT2014 software, and the dataset was TSP-normalized, generalized logarithmically (glog)-transformed and Pareto-scaled prior to analysis. Reproduced with permission from [140].

**DON'T FORGET THE CONCLUSION, PERSPECTIVES? ☺**

## ACKNOWLEDGMENTS

TCC acknowledges ANR (DEVIL_INSID project, grant ANR-18-CE39-0013-01 of the French National Research Agency.

DB acknowledges the Region Pays de la Loire ("Pari Scientifique Régional AMER-METAL") and the

French National Center for Scientific Research ("Osez l'Interdisciplinarité !" RMN-(ME)2-TAL)

JF thanks his partner Sandrine Bouchet for an unfailing assistance.

Bibliography:

[1] L. Banci, L. Barbieri, V. Calderone, F. Cantini, L. Cerofolini, S. Ciofi-Baffoni, I.C. Felli, M. Fragai, M. Lelli, C. Luchinat, E. Luchinat, G. Parigi, M. Piccioli, R. Pierattelli, E. Ravera, A. Rosato, L. Tenori, P. Turano, Biomolecular NMR at 1.2 GHz, ArXiv:1910.07462 [Physics]. (2019). http://arxiv.org/abs/1910.07462 (accessed October 14, 2020).

[2] W.R. de Araujo, T.M.G. Cardoso, R.G. da Rocha, M.H.P. Santana, R.A.A. Muñoz, E.M. Richter, T.R.L.C. Paixão, W.K.T. Coltro, Portable analytical platforms for forensic chemistry: A review, Anal Chim Acta. 1034 (2018) 1–21. https://doi.org/10.1016/j.aca.2018.06.014.

[3] R. Pilot, SERS detection of food contaminants by means of portable Raman instruments, Journal of Raman Spectroscopy. 49 (2018) 954–981. https://doi.org/10.1002/jrs.5400.

[4] C.R. Ferreira, K.E. Yannell, A.K. Jarmusch, V. Pirro, Z. Ouyang, R.G. Cooks, Ambient Ionization Mass Spectrometry for Point-of-Care Diagnostics and Other Clinical Measurements, Clin Chem. 62 (2016) 99–110. https://doi.org/10.1373/clinchem.2014.237164.

[5] E. Kırtıl, H Nuclear Magnetic Resonance Relaxometry and Magnetic Resonance Imaging and Applications in Food Science and Processing, 8 (2016) 1–22.

[6] R.M. Steele, J.-P. Korb, G. Ferrante, S. Bubici, New applications and perspectives of fast field cycling NMR relaxometry, Magnetic Resonance in Chemistry. 54 (2016) 502–509. https://doi.org/10.1002/mrc.4220.

[7] R. Kausik, K. Fellah, E. Rylander, P.M. Singer, R.E. Lewis, S.M. Sinclair, NMR Relaxometry in Shale and Implications for Logging, Petrophysics. 57 (2016) 339–350.

[8] S.K. Küster, E. Danieli, B. Blümich, F. Casanova, High-resolution NMR spectroscopy under the fume hood, Phys. Chem. Chem. Phys. 13 (2011) 13172–13176. https://doi.org/10.1039/C1CP21180C.

[9] K. Singh, B. Blümich, NMR spectroscopy with compact instruments, TrAC Trends in Analytical Chemistry. 83 (2016) 12–26. https://doi.org/10.1016/j.trac.2016.02.014.

[10] P. Giraudeau, F.-X. Felpin, Flow reactors integrated with in-line monitoring using benchtop NMR spectroscopy, React. Chem. Eng. 3 (2018) 399–413. https://doi.org/10.1039/C8RE00083B.

[11] D. Bouillaud, J. Farjon, O. Gonçalves, P. Giraudeau, Benchtop NMR for the monitoring of bioprocesses, Magnetic Resonance in Chemistry. 57 (2019) 794–804. https://doi.org/10.1002/mrc.4821.

[12] G. Assemat, S. Balayssac, A. Gerdova, V. Gilard, C. Caillet, D. Williamson, M. Malet-Martino, Benchtop low-field 1H Nuclear Magnetic Resonance for detecting falsified medicines, Talanta. 196 (2019) 163–173. https://doi.org/10.1016/j.talanta.2018.12.005.

[13] B. Gouilleux, J. Marchand, B. Charrier, G.S. Remaud, P. Giraudeau, High-throughput authentication of edible oils with benchtop Ultrafast 2D NMR, Food Chemistry. 244 (2018) 153–158. https://doi.org/10.1016/j.foodchem.2017.10.016.
[14] S.D. Riegel, G.M. Leskowitz, Benchtop NMR spectrometers in academic teaching, TrAC Trends in Analytical Chemistry. 83 (2016) 27–38. https://doi.org/10.1016/j.trac.2016.01.001.
[15] Fourier 80: Benchtop NMR from Bruker, (n.d.). https://www.bruker.com/products/mr/nmr/benchtop-nmr.html/ (accessed October 16, 2020).
[16] Which Benchtop NMR is right for you?, (n.d.). https://www.nanalysis.com/products-overview/ (accessed October 16, 2020).
[17] Spectromètre RMN picoSpin™ 80 série II, (n.d.). https://www.thermofisher.com/order/catalog/product/912A0913#/912A0913 (accessed October 16, 2020).
[18] Discover the Spinsolve family, (n.d.). http://www.magritek.com/products/spinsolve/ (accessed October 16, 2020).
[19] Welcome to Magnetic Resonance, (n.d.). https://nmr.oxinst.com/ (accessed October 16, 2020).
[20] E. Danieli, J. Perlo, A.L.L. Duchateau, G.K.M. Verzijl, V.M. Litvinov, B. Blümich, F. Casanova, On-Line Monitoring of Chemical Reactions by using Bench-Top Nuclear Magnetic Resonance Spectroscopy, ChemPhysChem. 15 (2014) 3060–3066. https://doi.org/10.1002/cphc.201402049.
[21] H. Raich, P. Blümler, Design and construction of a dipolar Halbach array with a homogeneous field from identical bar magnets: NMR Mandhalas, Concepts in Magnetic Resonance Part B: Magnetic Resonance Engineering. 23B (2004) 16–25. https://doi.org/10.1002/cmr.b.20018.
[22] E. Danieli, J. Mauler, J. Perlo, B. Blümich, F. Casanova, Mobile sensor for high resolution NMR spectroscopy and imaging, Journal of Magnetic Resonance. 198 (2009) 80–87. https://doi.org/10.1016/j.jmr.2009.01.022.
[23] B. Blümich, Introduction to compact NMR: A review of methods, TrAC Trends in Analytical Chemistry. 83 (2016) 2–11. https://doi.org/10.1016/j.trac.2015.12.012.
[24] E. Danieli, J. Perlo, B. Blümich, F. Casanova, Small Magnets for Portable NMR Spectrometers, Angewandte Chemie International Edition. 49 (2010) 4133–4135. https://doi.org/10.1002/anie.201000221.
[25] G.N. Chmurny, D.I. Hoult, The Ancient and Honourable Art of Shimming, Concepts in Magnetic Resonance. 2 (1990) 131–149. https://doi.org/10.1002/cmr.1820020303.
[26] K. Heerah, S. Waclawek, J. Konzuk, J.G. Longstaffe, Benchtop 19F NMR spectroscopy as a practical tool for testing of remedial technologies for the degradation of perfluorooctanoic acid, a persistent organic pollutant, Magnetic Resonance in Chemistry. (2020) 1–8. https://doi.org/10.1002/mrc.5005.
[27] N. Zientek, C. Laurain, K. Meyer, M. Kraume, G. Guthausen, M. Maiwald, Simultaneous 19F–1H medium resolution NMR spectroscopy for online reaction monitoring, Journal of Magnetic Resonance. 249 (2014) 53–62. https://doi.org/10.1016/j.jmr.2014.10.007.
[28] B. Gouilleux, N.V. Christensen, K.G. Malmos, T. Vosegaard, Analytical Evaluation of Low-Field 31P NMR Spectroscopy for Lipid Analysis, Anal. Chem. 91 (2019) 3035–3042. https://doi.org/10.1021/acs.analchem.8b05416.
[29] K.G. Malmos, B. Gouilleux, P. Sønderskov, T. Andersen, J.V. Frambøl, T. Vosegaard, Quantification of Ammonium Phosphatide Emulsifiers in Chocolate Using 31P NMR Spectroscopy, J. Agric. Food Chem. 66 (2018) 10309–10316. https://doi.org/10.1021/acs.jafc.8b04379.
[30] B. Bogun, S. Moore, 1H and 31P benchtop NMR of liquids and solids used in and/or produced during the manufacture of methamphetamine by the HI reduction of pseudoephedrine/ephedrine, Forensic Science International. 278 (2017) 68–77. https://doi.org/10.1016/j.forsciint.2017.06.026.
[31] G.M. Bernard, V.K. Michaelis, Lead-207 NMR spectroscopy at 1.4 T: Application of benchtop instrumentation to a challenging I = ½ nucleus, Magnetic Resonance in Chemistry. (2020) 1–10. https://doi.org/10.1002/mrc.5036.

[32] B. Gouilleux, B. Charrier, S. Akoka, P. Giraudeau, Gradient-based solvent suppression methods on a benchtop spectrometer, Magnetic Resonance in Chemistry. 55 (2017) 91–98. https://doi.org/10.1002/mrc.4493.
[33] T. Castaing-Cordier, D. Bouillaud, P. Bowyer, O. Gonçalves, P. Giraudeau, J. Farjon, Highly Resolved Pure-Shift Spectra on a Compact NMR Spectrometer, ChemPhysChem. 20 (2019) 736–744. https://doi.org/10.1002/cphc.201801116.
[34] B. Gouilleux, B. Charrier, S. Akoka, F.-X. Felpin, M. Rodriguez-Zubiri, P. Giraudeau, Ultrafast 2D NMR on a benchtop spectrometer: Applications and perspectives, TrAC Trends in Analytical Chemistry. 83 (2016) 65–75. https://doi.org/10.1016/j.trac.2016.01.014.
[35] G. Assemat, B. Gouilleux, D. Bouillaud, J. Farjon, V. Gilard, P. Giraudeau, M. Malet-Martino, Diffusion-ordered spectroscopy on a benchtop spectrometer for drug analysis, Journal of Pharmaceutical and Biomedical Analysis. 160 (2018) 268–275. https://doi.org/10.1016/j.jpba.2018.08.011.
[36] T.A. van Beek, Low-field benchtop NMR spectroscopy: status and prospects in natural product analysis, Phytochemical Analysis. (2020) 1–14. https://doi.org/10.1002/pca.2921.
[37] R. Cahill, T.A. Crabb, The 1H NMR spectra and conformations of some substituted morpholin-2-ones, Tetrahedron. 25 (1969) 1513–1521. https://doi.org/10.1016/S0040-4020(01)82724-1.
[38] K. Singh, S.P. Kumar, B. Blümich, Monitoring the mechanism and kinetics of a transesterification reaction for the biodiesel production with low field 1H NMR spectroscopy, Fuel. 243 (2019) 192–201. https://doi.org/10.1016/j.fuel.2019.01.084.
[39] K. Meyer, S. Kern, N. Zientek, G. Guthausen, M. Maiwald, Process control with compact NMR, TrAC Trends in Analytical Chemistry. 83 (2016) 39–52. https://doi.org/10.1016/j.trac.2016.03.016.
[40] Y. Lee, Y. Matviychuk, D.J. Holland, Quantitative analysis using external standards with a benchtop NMR spectrometer, Journal of Magnetic Resonance. 320 (2020) 106826. https://doi.org/10.1016/j.jmr.2020.106826.
[41] D.A. Armbruster, T. Pry, Limit of Blank, Limit of Detection and Limit of Quantitation, Clin Biochem Rev. 29 (2008) S49–S52.
[42] A. Krunić, J. Orjala, Application of high-field NMR spectroscopy for characterization and quantitation of submilligram quantities of isolated natural products, Magn Reson Chem. 53 (2015) 1043–1050. https://doi.org/10.1002/mrc.4304.
[43] G. Pagès, A. Gerdova, D. Williamson, V. Gilard, R. Martino, M. Malet-Martino, Evaluation of a Benchtop Cryogen-Free Low-Field 1H NMR Spectrometer for the Analysis of Sexual Enhancement and Weight Loss Dietary Supplements Adulterated with Pharmaceutical Substances, Anal. Chem. 86 (2014) 11897–11904. https://doi.org/10.1021/ac503699u.
[44] C. Zhang, T. Zhang, N.A. Oyler, B.-B.C. Youan, Direct and real-time quantification of tenofovir release from pH-sensitive microparticles into simulated biological fluids using 1H-NMR, J Pharm Sci. 103 (2014) 1170–1177.
[45] A.-H. Emwas, R. Roy, R.T. McKay, L. Tenori, E. Saccenti, G.A.N. Gowda, D. Raftery, F. Alahmari, L. Jaremko, M. Jaremko, D.S. Wishart, NMR Spectroscopy for Metabolomics Research, Metabolites. 9 (2019) 123. https://doi.org/10.3390/metabo9070123.
[46] B. Blümich, K. Singh, Desktop NMR and Its Applications From Materials Science To Organic Chemistry, Angewandte Chemie International Edition. 57 (2018) 6996–7010. https://doi.org/10.1002/anie.201707084.
[47] D.I. Hoult, Solvent peak saturation with single phase and quadrature fourier transformation, Journal of Magnetic Resonance (1969). 21 (1976) 337–347. https://doi.org/10.1016/0022-2364(76)90081-0.
[48] S.H. Smallcombe, S.L. Patt, P.A. Keifer, WET Solvent Suppression and Its Applications to LC NMR and High-Resolution NMR Spectroscopy, Journal of Magnetic Resonance, Series A. 117 (1995) 295–303. https://doi.org/10.1006/jmra.1995.0759.
[49] R.T. Mckay, How the 1D-NOESY suppresses solvent signal in metabonomics NMR spectroscopy: An examination of the pulse sequence components and evolution, Concepts in Magnetic Resonance Part A. 38A (2011) 197–220. https://doi.org/10.1002/cmr.a.20223.

[50] M. Piotto, V. Saudek, V. Sklenář, Gradient-tailored excitation for single-quantum NMR spectroscopy of aqueous solutions, J Biomol NMR. 2 (1992) 661–665. https://doi.org/10.1007/BF02192855.
[51] V.V. Krishnan, N. Murali, Radiation damping in modern NMR experiments: Progress and challenges, Prog Nucl Magn Reson Spectrosc. 68 (2013) 41–57. https://doi.org/10.1016/j.pnmrs.2012.06.001.
[52] H. Mo, D. Raftery, Pre-SAT180, a Simple and Effective Method for Residual Water Suppression, J Magn Reson. 190 (2008) 1–6. https://doi.org/10.1016/j.jmr.2007.09.016.
[53] P. Giraudeau, V. Silvestre, S. Akoka, Optimizing water suppression for quantitative NMR-based metabolomics: a tutorial review, Metabolomics. (2015). https://doi.org/10.1007/s11306-015-0794-7.
[54] T.L. Hwang, A.J. Shaka, Water Suppression That Works. Excitation Sculpting Using Arbitrary Wave-Forms and Pulsed-Field Gradients, Journal of Magnetic Resonance, Series A. 112 (1995) 275–279. https://doi.org/10.1006/jmra.1995.1047.
[55] D. Bouillaud, V. Heredia, T. Castaing-Cordier, D. Drouin, B. Charrier, O. Gonçalves, J. Farjon, P. Giraudeau, Benchtop flow NMR spectroscopy as an online device for the in vivo monitoring of lipid accumulation in microalgae, Algal Research. 43 (2019) 101624. https://doi.org/10.1016/j.algal.2019.101624.
[56] B. Picard, B. Gouilleux, T. Lebleu, J. Maddaluno, I. Chataigner, M. Penhoat, F.-X. Felpin, P. Giraudeau, J. Legros, Oxidative Neutralization of Mustard-Gas Simulants in an On-Board Flow Device with In-Line NMR Monitoring, Angewandte Chemie International Edition. 56 (2017) 7568–7572. https://doi.org/10.1002/anie.201702744.
[57] C. Botha, J. Höpfner, B. Mayerhöfer, M. Wilhelm, On-line SEC-MR-NMR hyphenation: optimization of sensitivity and selectivity on a 62 MHz benchtop NMR spectrometer, Polym. Chem. 10 (2019) 2230–2246. https://doi.org/10.1039/C9PY00140A.
[58] J. Höpfner, K.-F. Ratzsch, C. Botha, M. Wilhelm, Medium Resolution 1H-NMR at 62 MHz as a New Chemically Sensitive Online Detector for Size-Exclusion Chromatography (SEC–NMR), Macromolecular Rapid Communications. 39 (2018) 1700766. https://doi.org/10.1002/marc.201700766.
[59] C.S.J. Jr, ChemInform Abstract: Diffusion Ordered Nuclear Magnetic Resonance Spectroscopy: Principles and Applications, ChemInform. 30 (1999). https://doi.org/10.1002/chin.199933338.
[60] G. Pagès, V. Gilard, R. Martino, M. Malet-Martino, Pulsed-field gradient nuclear magnetic resonance measurements (PFG NMR) for diffusion ordered spectroscopy (DOSY) mapping, Analyst. 142 (2017) 3771–3796. https://doi.org/10.1039/C7AN01031A.
[61] L. Castañar, G.D. Poggetto, A.A. Colbourne, G.A. Morris, M. Nilsson, The GNAT: A new tool for processing NMR data, Magnetic Resonance in Chemistry. 56 (2018) 546–558. https://doi.org/10.1002/mrc.4717.
[62] A. Botana, J.A. Aguilar, M. Nilsson, G.A. Morris, J-modulation effects in DOSY experiments and their suppression: The Oneshot45 experiment, Journal of Magnetic Resonance. 208 (2011) 270–278. https://doi.org/10.1016/j.jmr.2010.11.012.
[63] E.R. McCarney, R. Dykstra, P. Galvosas, Evaluation of benchtop NMR Diffusion Ordered Spectroscopy for small molecule mixture analysis, Magnetic Resonance Imaging. 56 (2019) 103–109. https://doi.org/10.1016/j.mri.2018.09.033.
[64] E.R. McCarney, C.J. Breaux, P.M. Rendle, Measurement of the hydrodynamic radii of PEE-G dendrons by diffusion spectroscopy on a benchtop NMR spectrometer, Magnetic Resonance in Chemistry. 58 (2020) 641–647. https://doi.org/10.1002/mrc.4997.
[65] M.A. Delsuc, T.E. Malliavin, Maximum Entropy Processing of DOSY NMR Spectra, Anal. Chem. 70 (1998) 2146–2148. https://doi.org/10.1021/ac9800715.
[66] A.A. Colbourne, G.A. Morris, M. Nilsson, Local Covariance Order Diffusion-Ordered Spectroscopy: A Powerful Tool for Mixture Analysis, J. Am. Chem. Soc. 133 (2011) 7640–7643. https://doi.org/10.1021/ja2004895.

[67] W. Windig, B. Antalek, Direct exponential curve resolution algorithm (DECRA): A novel application of the generalized rank annihilation method for a single spectral mixture data set with exponentially decaying contribution profiles, Chemometrics and Intelligent Laboratory Systems. 37 (1997) 241–254. https://doi.org/10.1016/S0169-7439(97)00028-2.
[68] J.-N. Dumez, Spatial encoding and spatial selection methods in high-resolution NMR spectroscopy, Progress in Nuclear Magnetic Resonance Spectroscopy. 109 (2018) 101–134. https://doi.org/10.1016/j.pnmrs.2018.08.001.
[69] L. Frydman, T. Scherf, A. Lupulescu, The acquisition of multidimensional NMR spectra within a single scan, PNAS. 99 (2002) 15858–15862. https://doi.org/10.1073/pnas.252644399.
[70] B. Gouilleux, L. Rouger, P. Giraudeau, Ultrafast Multi-dimensional NMR: Principles and Recent Applications, Emagres. 5 (2016) 913–922. https://doi.org/10.1002/9780470034590.emrstm1494.
[71] B. Gouilleux, L. Rouger, P. Giraudeau, Ultrafast 2D NMR: Methods and Applications, in: G. Webb (Ed.), ANNUAL REPORTS ON NMR SPECTROSCOPY, VOL 93, 2018: pp. 75–144. https://doi.org/10.1016/bs.arnmr.2017.08.003.
[72] J. Marchand, E. Martineau, Y. Guitton, G. Dervilly-Pinel, P. Giraudeau, Multidimensional NMR approaches towards highly resolved, sensitive and high-throughput quantitative metabolomics, Curr Opin Biotechnol. 43 (2017) 49–55. https://doi.org/10.1016/j.copbio.2016.08.004.
[73] B. Gouilleux, B. Charrier, E. Danieli, J.-N. Dumez, S. Akoka, F.-X. Felpin, M. Rodriguez-Zubiri, P. Giraudeau, Real-time reaction monitoring by ultrafast 2D NMR on a benchtop spectrometer, Analyst. 140 (2015) 7854–7858. https://doi.org/10.1039/C5AN01998B.
[74] K. Zangger, Pure shift NMR, Progress in Nuclear Magnetic Resonance Spectroscopy. 86–87 (2015) 1–20. https://doi.org/10.1016/j.pnmrs.2015.02.002.
[75] P. Mutzenhardt, F. Guenneau, D. Canet, A Procedure for Obtaining Pure Absorption 2D J-Spectra: Application to Quantitative Fully J-Decoupled Homonuclear NMR Spectra, Journal of Magnetic Resonance. 141 (1999) 312–321. https://doi.org/10.1006/jmre.1999.1889.
[76] K. Rachineni, V.M.R. Kakita, R.V. Hosur, Ultra-high resolution in low field tabletop NMR spectrometers, RSC Adv. 7 (2017) 49102–49104. https://doi.org/10.1039/C7RA09594E.
[77] L. Castañar, Pure shift 1H NMR: what is next?, Magnetic Resonance in Chemistry. 55 (2017) 47–53. https://doi.org/10.1002/mrc.4545.
[78] K.H. Hausser, D. Stehlik, Dynamic Nuclear Polarization in Liquids, in: J.S. Waugh (Ed.), Advances in Magnetic and Optical Resonance, Academic Press, 1968: pp. 79–139. https://doi.org/10.1016/B978-1-4832-3116-7.50010-2.
[79] R.W. Adams, J.A. Aguilar, K.D. Atkinson, M.J. Cowley, P.I.P. Elliott, S.B. Duckett, G.G.R. Green, I.G. Khazal, J. López-Serrano, D.C. Williamson, Reversible Interactions with para-Hydrogen Enhance NMR Sensitivity by Polarization Transfer, Science. 323 (2009) 1708–1711. https://doi.org/10.1126/science.1168877.
[80] B. Plainchont, P. Berruyer, J.-N. Dumez, S. Jannin, P. Giraudeau, Dynamic Nuclear Polarization Opens New Perspectives for NMR Spectroscopy in Analytical Chemistry, Anal Chem. 90 (2018) 3639–3650. https://doi.org/10.1021/acs.analchem.7b05236.
[81] T. Prisner, W. Köckenberger, Dynamic Nuclear Polarization: New Experimental and Methodology Approaches and Applications in Physics, Chemistry, Biology and Medicine, Appl Magn Reson. 34 (2008) 213–218. https://doi.org/10.1007/s00723-008-0137-1.
[82] Y. Lee, D.-Y. Lim, J.H. Shim, Overhauser dynamic nuclear polarization for benchtop NMR system using a permanent magnet of 1.56 T, Journal of the Korean Magnetic Resonance Society. 23 (2019) 81–86. https://doi.org/10.6564/JKMRS.2019.23.3.081.
[83] J.H. Ardenkjær-Larsen, B. Fridlund, A. Gram, G. Hansson, L. Hansson, M.H. Lerche, R. Servin, M. Thaning, K. Golman, Increase in signal-to-noise ratio of > 10,000 times in liquid-state NMR, PNAS. 100 (2003) 10158–10163. https://doi.org/10.1073/pnas.1733835100.
[84] S.J. Nelson, J. Kurhanewicz, D.B. Vigneron, P.E.Z. Larson, A.L. Harzstark, M. Ferrone, M. van Criekinge, J.W. Chang, R. Bok, I. Park, G. Reed, L. Carvajal, E.J. Small, P. Munster, V.K. Weinberg, J.H. Ardenkjaer-Larsen, A.P. Chen, R.E. Hurd, L.-I. Odegardstuen, F.J. Robb, J. Tropp, J.A. Murray, Metabolic Imaging of Patients with Prostate Cancer Using Hyperpolarized [1-13C]Pyruvate,

Science Translational Medicine. 5 (2013) 198ra108-198ra108. https://doi.org/10.1126/scitranslmed.3006070.
[85] S. Jannin, J.-N. Dumez, P. Giraudeau, D. Kurzbach, Application and methodology of dissolution dynamic nuclear polarization in physical, chemical and biological contexts, Journal of Magnetic Resonance. 305 (2019) 41–50. https://doi.org/10.1016/j.jmr.2019.06.001.
[86] S.S. Tee, V. DiGialleonardo, R. Eskandari, S. Jeong, K.L. Granlund, V. Miloushev, A.J. Poot, S. Truong, J.A. Alvarez, H.N. Aldeborgh, K.R. Keshari, Sampling Hyperpolarized Molecules Utilizing a 1 Tesla Permanent Magnetic Field, Scientific Reports. 6 (2016) 32846. https://doi.org/10.1038/srep32846.
[87] X. Ji, A. Bornet, B. Vuichoud, J. Milani, D. Gajan, A.J. Rossini, L. Emsley, G. Bodenhausen, S. Jannin, Transportable hyperpolarized metabolites, Nature Communications. 8 (2017) 13975. https://doi.org/10.1038/ncomms13975.
[88] null Bowers, null Weitekamp, Transformation of symmetrization order to nuclear-spin magnetization by chemical reaction and nuclear magnetic resonance, Phys Rev Lett. 57 (1986) 2645–2648. https://doi.org/10.1103/PhysRevLett.57.2645.
[89] D. Blazina, S.B. Duckett, J.P. Dunne, C. Godard, Applications of the parahydrogen phenomenon in inorganic chemistry, Dalton Trans. (2004) 2601–2609. https://doi.org/10.1039/B409606A.
[90] S. Korchak, S. Mamone, S. Glöggler, Over 50 % 1H and 13C Polarization for Generating Hyperpolarized Metabolites—A para-Hydrogen Approach, ChemistryOpen. 7 (2018) 672–676. https://doi.org/10.1002/open.201800086.
[91] L.S. Lloyd, R.W. Adams, M. Bernstein, S. Coombes, S.B. Duckett, G.G.R. Green, Richard.J. Lewis, R.E. Mewis, C.J. Sleigh, Utilization of SABRE-Derived Hyperpolarization To Detect Low-Concentration Analytes via 1D and 2D NMR Methods, J. Am. Chem. Soc. 134 (2012) 12904–12907. https://doi.org/10.1021/ja3051052.
[92] B.J. Tickner, P.J. Rayner, S.B. Duckett, Using SABRE Hyperpolarized 13C NMR Spectroscopy to Interrogate Organic Transformations of Pyruvate, Anal Chem. 92 (2020) 9095–9103. https://doi.org/10.1021/acs.analchem.0c01334.
[93] N. Eshuis, B.J.A. van Weerdenburg, M.C. Feiters, F.P.J.T. Rutjes, S.S. Wijmenga, M. Tessari, Quantitative Trace Analysis of Complex Mixtures Using SABRE Hyperpolarization, Angewandte Chemie International Edition. 54 (2015) 1481–1484. https://doi.org/10.1002/anie.201409795.
[94] M.E. Halse, Perspectives for hyperpolarisation in compact NMR, TrAC Trends in Analytical Chemistry. 83 (2016) 76–83. https://doi.org/10.1016/j.trac.2016.05.004.
[95] J.-B. Hövener, S. Knecht, N. Schwaderlapp, J. Hennig, D. von Elverfeldt, Continuous Re-hyperpolarization of Nuclear Spins Using Parahydrogen: Theory and Experiment, ChemPhysChem. 15 (2014) 2451–2457. https://doi.org/10.1002/cphc.201402177.
[96] B. Joalland, A.B. Schmidt, M.S.H. Kabir, N.V. Chukanov, K.V. Kovtunov, I.V. Koptyug, J. Hennig, J.-B. Hövener, E.Y. Chekmenev, Pulse-Programmable Magnetic Field Sweeping of Parahydrogen-Induced Polarization by Side Arm Hydrogenation, Anal. Chem. 92 (2020) 1340–1345. https://doi.org/10.1021/acs.analchem.9b04501.
[97] S. Lehmkuhl, M. Wiese, L. Schubert, M. Held, M. Küppers, M. Wessling, B. Blümich, Continuous hyperpolarization with parahydrogen in a membrane reactor, Journal of Magnetic Resonance. 291 (2018) 8–13. https://doi.org/10.1016/j.jmr.2018.03.012.
[98] K. Jeong, S. Min, H. Chae, S.K. Namgoong, Monitoring of hydrogenation by benchtop NMR with parahydrogen-induced polarization, Magnetic Resonance in Chemistry. 57 (2019) 44–48. https://doi.org/10.1002/mrc.4791.
[99] D. Gołowicz, K. Kazimierczuk, M. Urbańczyk, T. Ratajczyk, Monitoring Hydrogenation Reactions using Benchtop 2D NMR with Extraordinary Sensitivity and Spectral Resolution, ChemistryOpen. 8 (2019) 196–200. https://doi.org/10.1002/open.201800294.
[100] A.D. Robinson, P.M. Richardson, M.E. Halse, Hyperpolarised 1H-13C benchtop NMR spectroscopy, Applied Sciences. (2019). http://eprints.whiterose.ac.uk/143732/ (accessed February 19, 2020).

[101] A.W.J. Logan, T. Theis, J.F.P. Colell, W.S. Warren, S.J. Malcolmson, Hyperpolarization of Nitrogen-15 Schiff Bases by Reversible Exchange Catalysis with para-Hydrogen, Chemistry – A European Journal. 22 (2016) 10777–10781. https://doi.org/10.1002/chem.201602393.
[102] J.F.P. Colell, A.W.J. Logan, Z. Zhou, R.V. Shchepin, D.A. Barskiy, G.X. Ortiz, Q. Wang, S.J. Malcolmson, E.Y. Chekmenev, W.S. Warren, T. Theis, Generalizing, Extending, and Maximizing Nitrogen-15 Hyperpolarization Induced by Parahydrogen in Reversible Exchange, J. Phys. Chem. C. 121 (2017) 6626–6634. https://doi.org/10.1021/acs.jpcc.6b12097.
[103] L. Chen, Z. Weng, L. Goh, M. Garland, An efficient algorithm for automatic phase correction of NMR spectra based on entropy minimization, Journal of Magnetic Resonance. 158 (2002) 164–168. https://doi.org/10.1016/S1090-7807(02)00069-1.
[104] Q. Bao, J. Feng, L. Chen, F. Chen, Z. Liu, B. Jiang, C. Liu, A robust automatic phase correction method for signal dense spectra, Journal of Magnetic Resonance. 234 (2013) 82–89. https://doi.org/10.1016/j.jmr.2013.06.012.
[105] M. a. R. Anjum, P.A. Dmochowski, P.D. Teal, A subband Steiglitz-McBride algorithm for automatic analysis of FID data, Magnetic Resonance in Chemistry. 56 (2018) 740–747. https://doi.org/10.1002/mrc.4723.
[106] Y. Matviychuk, E. von Harbou, D.J. Holland, An experimental validation of a Bayesian model for quantification in NMR spectroscopy, Journal of Magnetic Resonance. 285 (2017) 86–100. https://doi.org/10.1016/j.jmr.2017.10.009.
[107] M. Sawall, E. von Harbou, A. Moog, R. Behrens, H. Schröder, J. Simoneau, E. Steimers, K. Neymeyr, Multi-objective optimization for an automated and simultaneous phase and baseline correction of NMR spectral data, Journal of Magnetic Resonance. 289 (2018) 132–141. https://doi.org/10.1016/j.jmr.2018.02.012.
[108] S.K. Bharti, R. Roy, Quantitative 1H NMR spectroscopy, TrAC Trends in Analytical Chemistry. 35 (2012) 5–26. https://doi.org/10.1016/j.trac.2012.02.007.
[109] L. Miloudi, F. Bonnier, K. Barreau, D. Bertrand, X. Perse, F. Yvergnaux, H.J. Byrne, I. Chourpa, E. Munnier, ATR-IR coupled to partial least squares regression (PLSR) for monitoring an encapsulated active molecule in complex semi-solid formulations, Analyst. 143 (2018) 2377–2389. https://doi.org/10.1039/C8AN00547H.
[110] B. Worley, R. Powers, Multivariate Analysis in Metabolomics, Curr Metabolomics. 1 (2013) 92–107. https://doi.org/10.2174/2213235X11301010092.
[111] S. Kern, K. Meyer, S. Guhl, P. Gräßer, A. Paul, R. King, M. Maiwald, Online low-field NMR spectroscopy for process control of an industrial lithiation reaction—automated data analysis, Anal Bioanal Chem. 410 (2018) 3349–3360. https://doi.org/10.1007/s00216-018-1020-z.
[112] Y. Matviychuk, J. Yeo, D.J. Holland, A field-invariant method for quantitative analysis with benchtop NMR, Journal of Magnetic Resonance. 298 (2019) 35–47. https://doi.org/10.1016/j.jmr.2018.11.010.
[113] G.F. Pauli, qNMR--a versatile concept for the validation of natural product reference compounds, Phytochem Anal. 12 (2001) 28–42. https://doi.org/10.1002/1099-1565(200101/02)12:1<28::AID-PCA549>3.0.CO;2-D.
[114] P. Giraudeau, Challenges and perspectives in quantitative NMR, Magnetic Resonance in Chemistry. 55 (2017) 61–69. https://doi.org/10.1002/mrc.4475.
[115] D.A. Foley, A.L. Dunn, M.T. Zell, Reaction monitoring using online vs tube NMR spectroscopy: seriously different results, Magnetic Resonance in Chemistry. 54 (2016) 451–456. https://doi.org/10.1002/mrc.4259.
[116] K. Singh, E. Danieli, B. Blümich, Desktop NMR spectroscopy for real-time monitoring of an acetalization reaction in comparison with gas chromatography and NMR at 9.4 T, Anal Bioanal Chem. 409 (2017) 7223–7234. https://doi.org/10.1007/s00216-017-0686-y.
[117] A. Friebel, T. Specht, E. von Harbou, K. Münnemann, H. Hasse, Prediction of flow effects in quantitative NMR measurements, Journal of Magnetic Resonance. 312 (2020) 106683. https://doi.org/10.1016/j.jmr.2020.106683.

[118] A. Soyler, D. Bouillaud, J. Farjon, P. Giraudeau, M.H. Oztop, Real-time benchtop NMR spectroscopy for the online monitoring of sucrose hydrolysis, LWT. 118 (2020) 108832. https://doi.org/10.1016/j.lwt.2019.108832.
[119] V. Sans, L. Porwol, V. Dragone, L. Cronin, A self optimizing synthetic organic reactor system using real-time in-line NMR spectroscopy, Chem. Sci. 6 (2015) 1258–1264. https://doi.org/10.1039/C4SC03075C.
[120] T.H. Rehm, C. Hofmann, D. Reinhard, H.-J. Kost, P. Löb, M. Besold, K. Welzel, J. Barten, A. Didenko, D.V. Sevenard, B. Lix, A.R. Hillson, S.D. Riegel, Continuous-flow synthesis of fluorine-containing fine chemicals with integrated benchtop NMR analysis, React. Chem. Eng. 2 (2017) 315–323. https://doi.org/10.1039/C7RE00023E.
[121] W.G. Lee, M.T. Zell, T. Ouchi, M.J. Milton, NMR spectroscopy goes mobile: Using NMR as process analytical technology at the fume hood, Magnetic Resonance in Chemistry. (2020) 1–10. https://doi.org/10.1002/mrc.5035.
[122] N. Nestle, Z.J. Lim, T. Böhringer, S. Abtmeyer, S. Arenz, F.C. Leinweber, T. Weiß, E. von Harbou, Taking compact NMR to monitoring real reactions in large-scale chemical industries—General considerations and learnings from a lab-scale test case, Magnetic Resonance in Chemistry. (2020) 1–9. https://doi.org/10.1002/mrc.5061.
[123] D. Cortés-Borda, E. Wimmer, B. Gouilleux, E. Barré, N. Oger, L. Goulamaly, L. Peault, B. Charrier, C. Truchet, P. Giraudeau, M. Rodriguez-Zubiri, E. Le Grognec, F.-X. Felpin, An Autonomous Self-Optimizing Flow Reactor for the Synthesis of Natural Product Carpanone, J. Org. Chem. 83 (2018) 14286–14299. https://doi.org/10.1021/acs.joc.8b01821.
[124] D. Kreyenschulte, E. Paciok, L. Regestein, B. Blümich, J. Büchs, Online monitoring of fermentation processes via non-invasive low-field NMR, Biotechnology and Bioengineering. 112 (2015) 1810–1821. https://doi.org/10.1002/bit.25599.
[125] D. Bouillaud, D. Drouin, B. Charrier, C. Jacquemmoz, J. Farjon, P. Giraudeau, O. Gonçalves, Using benchtop NMR spectroscopy as an online non-invasive in vivo lipid sensor for microalgae cultivated in photobioreactors, Process Biochemistry. 93 (2020) 63–68. https://doi.org/10.1016/j.procbio.2020.03.016.
[126] S.D. Riegel, Determination of olive oil adulteration with 60-MHz benchtop NMR spectrometry, American Laboratory. 48 (2015) 16–19.
[127] T. Parker, E. Limer, A.D. Watson, M. Defernez, D. Williamson, E.K. Kemsley, 60MHz 1H NMR spectroscopy for the analysis of edible oils, TrAC Trends in Analytical Chemistry. 57 (2014) 147–158. https://doi.org/10.1016/j.trac.2014.02.006.
[128] J.H. Kim, H.J. Lee, K. Kwon, H.S. Chun, S. Ahn, B.H. Kim, A 43 MHz Low-Field Benchtop 1H Nuclear Magnetic Resonance Method to Discriminate Perilla Oil Authenticity, Journal of Oleo Science. 67 (2018) 507–513. https://doi.org/10.5650/jos.ess17243.
[129] D. McDowell, M. Defernez, E.K. Kemsley, C.T. Elliott, A. Koidis, Low vs high field 1h Nmr spectroscopy for the detection of adulteration of cold pressed rapeseed oil with refined oils, LWT. 111 (2019) 490–499. https://doi.org/10.1016/j.lwt.2019.05.065.
[130] W. Jakes, A. Gerdova, M. Defernez, A.D. Watson, C. McCallum, E. Limer, I.J. Colquhoun, D.C. Williamson, E.K. Kemsley, Authentication of beef versus horse meat using 60MHz 1H NMR spectroscopy, Food Chemistry. 175 (2015) 1–9. https://doi.org/10.1016/j.foodchem.2014.11.110.
[131] Y. Gunning, M. Defernez, A.D. Watson, N. Beadman, I.J. Colquhoun, G. Le Gall, M. Philo, H. Garwood, D. Williamson, A.P. Davis, E.K. Kemsley, 16-O-methylcafestol is present in ground roast Arabica coffees: Implications for authenticity testing, Food Chemistry. 248 (2018) 52–60. https://doi.org/10.1016/j.foodchem.2017.12.034.
[132] Y.B. Monakhova, W. Ruge, T. Kuballa, M. Ilse, O. Winkelmann, B. Diehl, F. Thomas, D.W. Lachenmeier, Rapid approach to identify the presence of Arabica and Robusta species in coffee using 1H NMR spectroscopy, Food Chemistry. 182 (2015) 178–184. https://doi.org/10.1016/j.foodchem.2015.02.132.

[133] K. Singh, B. Blümich, Compact low-field NMR spectroscopy and chemometrics: A tool box for quality control of raw rubber, Polymer. 141 (2018) 154–165. https://doi.org/10.1016/j.polymer.2018.02.057.
[134] A. Zivkovic, J.J. Bandolik, A.J. Skerhut, C. Coesfeld, M. Prascevic, L. Zivkovic, H. Stark, Quantitative Analysis of Multicomponent Mixtures of Over-the-Counter Pain Killer Drugs by Low-Field NMR Spectroscopy, J. Chem. Educ. 94 (2017) 121–125. https://doi.org/10.1021/acs.jchemed.6b00105.
[135] G. Assemat, F. Dubocq, S. Balayssac, C. Lamoureux, M. Malet-Martino, V. Gilard, Screening of "spice" herbal mixtures: From high-field to low-field proton NMR, Forensic Science International. 279 (2017) 88–95. https://doi.org/10.1016/j.forsciint.2017.08.006.
[136] L.H. Antonides, R.M. Brignall, A. Costello, J. Ellison, S.E. Firth, N. Gilbert, B.J. Groom, S.J. Hudson, M.C. Hulme, J. Marron, Z.A. Pullen, T.B.R. Robertson, C.J. Schofield, D.C. Williamson, E.K. Kemsley, O.B. Sutcliffe, R.E. Mewis, Rapid Identification of Novel Psychoactive and Other Controlled Substances Using Low-Field 1H NMR Spectroscopy, ACS Omega. 4 (2019) 7103–7112. https://doi.org/10.1021/acsomega.9b00302.
[137] Y. Zhong, K. Huang, Q. Luo, S. Yao, X. Liu, N. Yang, C. Lin, X. Luo, The Application of a Desktop NMR Spectrometer in Drug Analysis, International Journal of Analytical Chemistry. (2018). https://doi.org/10.1155/2018/3104569.
[138] J. Duffy, A. Urbas, M. Niemitz, K. Lippa, I. Marginean, Differentiation of fentanyl analogues by low-field NMR spectroscopy, Analytica Chimica Acta. 1049 (2019) 161–169. https://doi.org/10.1016/j.aca.2018.12.014.
[139] P. Giraudeau, NMR-based metabolomics and fluxomics: developments and future prospects, Analyst. 145 (2020) 2457–2472. https://doi.org/10.1039/D0AN00142B.
[140] B.C. Percival, M. Grootveld, M. Gibson, Y. Osman, M. Molinari, F. Jafari, T. Sahota, M. Martin, F. Casanova, M.L. Mather, M. Edgar, J. Masania, P.B. Wilson, Low-Field, Benchtop NMR Spectroscopy as a Potential Tool for Point-of-Care Diagnostics of Metabolic Conditions: Validation, Protocols and Computational Models, High Throughput. 8 (2018). https://doi.org/10.3390/ht8010002.